

1 **The development of a pregnancy PBPK Model for Bisphenol**
2 **A and its evaluation with the available biomonitoring data**

3
4
5 Raju Prasad Sharma, Marta Schuhmacher, Vikas Kumar*

6
7
8
9 *Center of Environmental Food and Toxicological Technology (TecnATox),*
10 *Departament d'Enginyeria Química, Universitat Rovira i Virgili, Tarragona,*
11 *Catalonia, Spain*

12
13
14 * Corresponding author: Environmental Engineering Laboratory, Departament
15 d'Enginyeria Química, Universitat Rovira i Virgili, Tarragona, Catalonia, Spain. Tel.:
16 +34977558576.

17 *E-mail address:* vikas.kumar@urv.cat
18
19

20 **Abstract**

21 Recent studies suggest universal fetal exposure to Bisphenol A (BPA) and its
22 association with the adverse birth outcomes. Estimation of the fetal plasma BPA
23 concentration from the maternal plasma BPA would be highly useful to predict its
24 associated risk to this specific population. The objective of current work is to develop a
25 pregnancy–physiologically based pharmacokinetic (P-PBPK) model to predict the
26 toxicokinetic profile of BPA in the fetus during gestational growth, and to evaluate the
27 developed model using biomonitoring data obtained from different pregnancy cohort
28 studies. To achieve this objective, first, the adult PBPK model was developed and
29 validated with the human BPA toxicokinetic data. This validated human PBPK model
30 was extended to develop a P-PBPK model, which included the physiological changes
31 during pregnancy and the fetus sub-model. The developed model would be able to
32 predict the BPA pharmacokinetics (PKs) in both mother and fetus. Transplacental BPA
33 kinetics parameters for this study were taken from the previous pregnant mice study.
34 Both oral and dermal exposure routes were included into the model to simulate total
35 BPA internal exposure. The impact of conjugation and deconjugation of the BPA and
36 its metabolites on fetal PKs was investigated. The developed P-PBPK model was
37 evaluated against the observed BPA concentrations in cord blood, fetus liver and
38 amniotic fluid considering maternal blood concentration as an exposure source. A
39 range of maternal exposure dose for the oral and dermal routes was estimated, so that
40 simulation concentration matched the observed highest and lowest mother plasma
41 concentration in different cohorts' studies. The developed model could be used to
42 address the concerns regarding possible adverse health effects in the fetus being
43 exposed to BPA and might be useful in identifying critical windows of exposure during
44 pregnancy.

45

46 **Key words:** Bisphenol A; pregnancy-PBPK; fetal exposure; biomonitoring;
47 window of exposure.

48 **1. Introduction**

49 BPA is produced at over 2 billion pounds/year and is found in wide variety of dietary
50 and non-dietary products. The dietary sources include both canned and non-canned
51 foods categories ranging from “meat and meat products”, “vegetables and vegetable
52 products”, and other packaged foods, and food handling consumer products like baby
53 bottles, beverage containers etc. (WHO, 2010; EFSA, 2015). The non-dietary sources
54 include medical devices, dental sealants, dust, thermal papers, toys and cosmetics
55 (Mendum et al., 2011; EFSA, 2015). Although ingestion of the BPA from food or water
56 is the predominant route of exposure (Lorber et al., 2015), there are other non-dietary
57 routes, which also equally contributes to the total BPA exposure, such as inhalation of
58 free BPA (concentrations in indoor and outdoor air), indirect ingestion (dust, soil, and
59 toys), and dermal route (contact with thermal papers and application of dental
60 treatment) (Myridakis et al., 2016). Recently reported studies have found relatively
61 more contribution of the dermal route to overall internal BPA concentration than the
62 oral route’s exposure (Biedermann et al., 2010; Mielke et al., 2011). In addition, recent
63 studies (De Coensel et al., 2009; Sungur et al., 2014) show that temperature has a
64 major impact on the BPA migration level into water; an increase from 40 °C to 60 °C
65 can lead to a 6 - 10 fold increase in the migration level.

66 BPA and its metabolites have been detected in maternal blood, amniotic fluid, follicular
67 fluid, placental tissue, umbilical cord blood, urine and breast milk (Schönfelder et al.,
68 2002; Ikezuki et al., 2002; Kuroda et al., 2003; Kuruto-Niwa et al., 2007; Lee et al.,
69 2008; Zhang et al., 2011,2013; Cao et al., 2012; Nahar et al., 2013; Gerona et al.,
70 2014; Teegarden et al., 2016). In different rodents’ studies, it has been seen that low
71 dose of bisphenol exposure during the gestational period has effects on the fertility,
72 brain development, and the behavioural changes in their later life stages, signify BPA
73 pleiotropic effects (Palanza et al., 2002; Cabaton et al., 2013; Snijder et al., 2013;
74 Harley et al., 2013). Rubin and Soto, (2009) reviewed the prenatal BPA exposure and
75 its effects on adipocytes differentiation, a major cause of obesity. U.S. Environmental
76 Protection Agency (EPA) has declared the BPA as an endocrine-modifying chemical,
77 which has been found to be reproductive, developmental, systemic toxicant,
78 obesogenic and, weakly estrogenic (Moriyama et al., 2002; Rey et al., 2003; Patisaul et
79 al., 2009; Xi et al., 2011; Wang et al., 2012; Vafeiadi et al., 2016; Sharma et al., 2016).

80 Adult human studies have reported that BPA has a very short half-life. It rapidly
81 detoxifies to nontoxic conjugate substance such as BPA-glucuronide (BPAG) and
82 BPA-sulfate (BPAS), collectively called as BPA conjugates (BPA-C), by glucuronidation

83 and sulfation metabolic process (Völkel et al., 2002; Teeguarden et al., 2015; Thayer et
84 al., 2015). However, in the case of the specific populations such as developing fetus,
85 growing infants, and young children, whose chemical metabolizing systems are
86 underdeveloped, even moderate exposure can lead to higher internal concentration of
87 BPA (Divakaran et al., 2014). Moreover, the reactivation of these conjugates
88 (deconjugation),BPAG and BPAS, by the fetal tissue and the placenta has been
89 reported(Ginsberg and Rice, 2009; Nahar et al., 2013),causing an increase in BPA
90 internal exposure to the fetus. The recent human pharmacokinetics studies showed low
91 amount of BPA plasma concentration even with the high oral dose, in contrast,
92 exposure amount of BPA for the different cohorts are estimated to be very low against
93 higher BPA plasma concentration obtained in biomonitoring studies (Völkel et al., 2005,
94 2002; Teeguarden et al., 2015; Thayer et al., 2015). Mielke and Gundert-Remy, (2009)
95 compared the observed biomonitoring data of Schönfelder et al., (2002) study against
96 the model predicted plasma concentrations of BPA using the simple kinetic approach
97 and physiological based pharmacokinetic (PBPK) model, and found 3000 fold lower
98 difference between the model prediction and the observed biomonitoring data. This
99 wide discrepancy between the pharmacokinetic models' prediction and the
100 biomonitoring data could be due to physiological variation, genetic polymorphisms
101 among populations, exposure variation and exclusion of non-oral routes of exposure.
102 However, the possible contamination during sample collection and analysis could be
103 one reason for this discrepancy (Longnecker et al., 2013; Ye et al., 2013) but it is
104 beyond the scope of this paper. Functional polymorphism in glucuronidation enzyme
105 responsible for the BPA metabolisms has been reported by Trdan Lusin et al., (2012).
106 It has been found that BPA after dermal exposure has a longer half -life of 8hr as it
107 bypass the first pass metabolism, and attains the steady state in blood by the 4th day,
108 whereas single oral dose intake completely eliminates in 6-8hr and never reach steady
109 state even with daily dosing (Biedermann et al., 2010; Mielke et al., 2011; Mielke and
110 Gundert-Remy, 2012; Gundert-Remy et al., 2013).

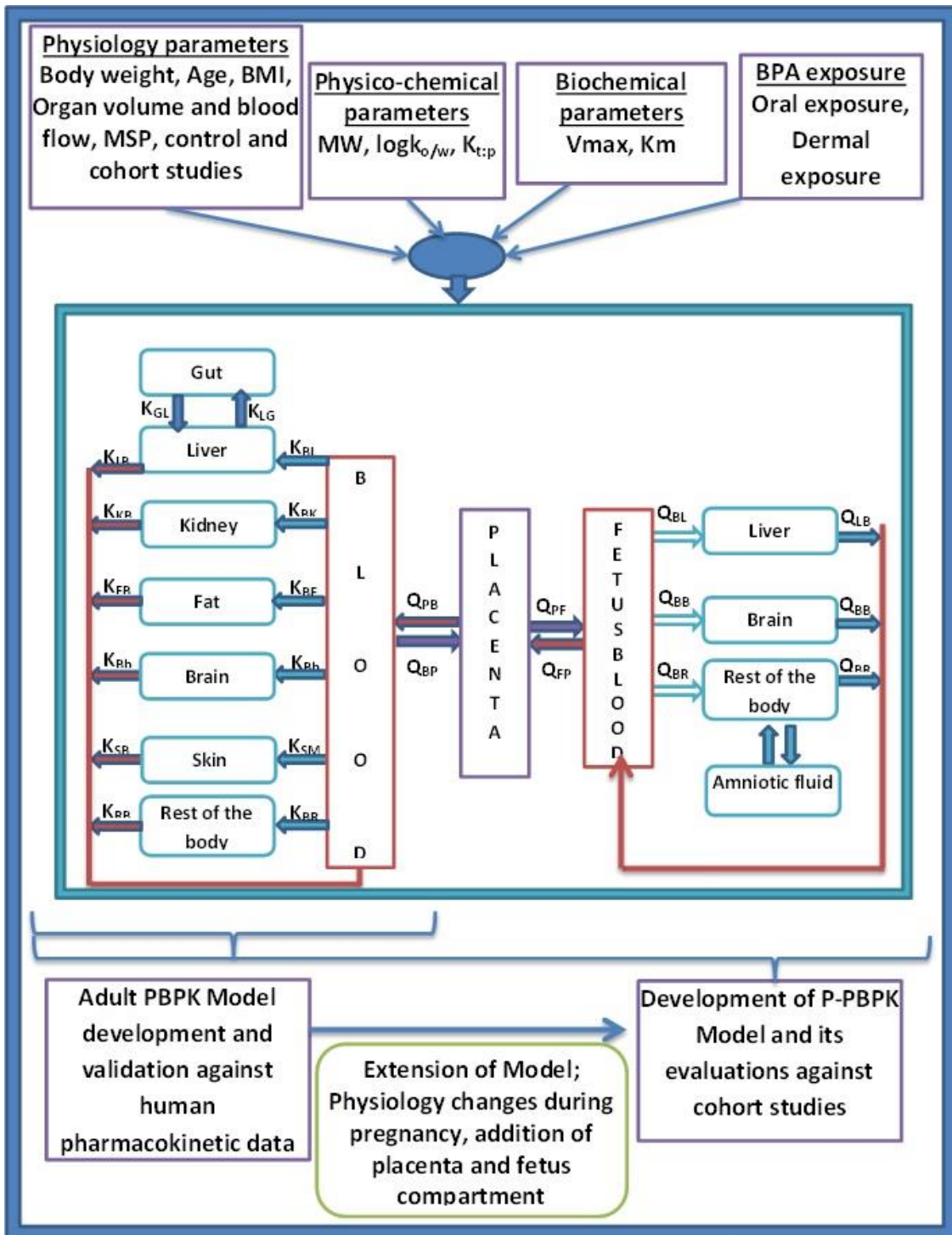
111 Previously, adult human, rat and monkey PBPK models have been developed for the
112 BPA and its conjugates (Shin et al., 2004; Edginton and Ritter, 2009; Fisher et al.,
113 2011; Yang et al., 2015, 2013; Yang and Fisher, 2015). The pregnancy
114 physiologically- based pharmacokinetic (P-PBPK) models have long been used to
115 estimate the exposure of the chemical to the fetus (Corley et al., 2003). The P-PBPK
116 model for mice was previously developed (Kawamoto et al., 2007), which showed the
117 potential exposure of BPA to the fetus. However, a P-PBPK model for the human has
118 not yet been developed. The pharmacokinetic data for chemicals are often limited in

119 specific populations of pregnant mother and fetus, due to the ethical and technical
120 reason, which often lead to difficulties in building a kinetic model. However, the use of
121 a physiological based pharmacokinetic model can simplify this complexity, based on its
122 capability to predict the kinetics of chemical via a mechanistic understanding of its
123 absorption, distribution, metabolisms, and elimination inside the body. The overall aim
124 of this study was to improve the understanding of the chemical toxicokinetic
125 relationship between the mother and the fetus by developing a P-PBPK model for the
126 BPA and its conjugates. This would enable to predict the fetus plasma and organs BPA
127 concentration by estimating the mother plasma BPA concentration and, thus helps in
128 identifying the critical window(s) of exposure to the fetus during its gestational period of
129 development. The conceptual model diagram is provided in Figure 1 showing the study
130 design undertaken for this work. The P-PBPK model development has followed
131 following phases: a) development and validation of the adult PBPK model, b) Extension
132 of the developed adult PBPK model to a P-PBPK with the inclusions of dynamic
133 physiological changes during the pregnancy and the prediction of chemical
134 toxicokinetic profile in both mother and fetus compartment and c) evaluation of
135 developed P-PBPK model against the biomonitoring data of available pregnant cohort
136 population. An additional case study of this model has been recently published in
137 Martínez et al., (2017), where simulation of prenatal BPA exposure via dietary intake of
138 pregnant women recruited from Tarragona county was performed.

139 **2. Methodology and parameterization**

140 Development of the P-PBPK model retains entire feature that used to describes the
141 adult BPA and BPA-C (BPAG and BPAS) kinetics like partition coefficient for the
142 organs, fraction unbound, metabolism (V_{max} and K_m) and elimination (urinary
143 elimination). The physiological changes that occur during pregnancy like changes in
144 plasma volume, fat volume, amniotic fluid, placental and fetal growth are described as
145 dynamic parameters that depend on the gestational period(Gentry et al., 2003;
146 Abduljalil et al., 2012). Besides the oral mode of exposure, dermal mode of exposure
147 was included in the development of the pregnancy-PBPK model. The oral exposure
148 was divided into three equal doses and dermal as a single dose. Considering the
149 gestational growth physiology in the case of the pregnant mother and fetus, the
150 development of a P-PBPK model has been described in the following section. The
151 models were coded in the R program (version 3.2.3), and model equations are
152 provided in the supplementary material (Annex-I).

153



154

155

156 Figure 1. A conceptual model for the development of P-PBPK model. It involves the
 157 development of the adult PBPK model and extension of this model to the P-PBPK
 158 model with the addition of placenta and fetus sub-compartment. MW = molecular
 159 weight, BMI = basal metabolic index, MSP = microsomal protein, K = partition

160 coefficient and subscripts L = Liver, B= blood, b = brain, K= kidney, S= skin, R= rest
161 organ, G= gut, Q = cardiac blood flow, P = placenta, F = fetus.

162

163 **2.1. General pregnancy-PBPK Model structure**

164 The basic structure of the P-PBPK model has been adapted from an adult model,
165 which included plasma, liver, kidneys, fat, brain, skin and a rest of the body
166 compartment for the remaining tissues. The placenta and the fetus compartments were
167 added into the model. The fetus compartment is further extended to fetus sub-model
168 considering liver, kidney, brain, and plasma as fetus sub-compartments. The fetus sub-
169 model considered the fetus-specific metabolic processes and included important target
170 organs for the prediction of internal target dosimetry. The physiological and metabolic
171 parameters were applied for the fetus model as dynamic parameters of gestational
172 period and chemical-specific parameters such as partition coefficient were kept similar
173 to the adult human model in the case of both Mother and fetus organs.

174

175 The source of exposure to the fetus was via unbound concentration of the chemical in
176 the mother placenta, assuming only the mother directly exposed to the chemical. The
177 placental-fetal unit assumes a bidirectional transfer process describing BPA and BPA-
178 G transfer between mother placenta to fetus plasma and vice versa. The transfer rate
179 was assumed as a simple diffusion process. Transport of chemical from fetal plasma
180 into the fetal compartments like liver, kidney, brain, and rest of the body was assumed
181 to be simple diffusion described by partition coefficient (same as of mother tissue). The
182 amniotic fluid compartment was included in the current P-PBPK model. Transfer rates
183 between the amniotic fluid compartment and the fetal body were described as a simple
184 diffusion process.

185 The elimination of BPA in the mother was assumed to be similar to adult human, which
186 occurs via its rapid metabolism in the liver and intestine, subsequently excreted via
187 urine. However, the clearance of BPA and its conjugates in the fetus was described
188 with first order transfer rate from fetus plasma to mother plasma via the placenta.

189 **2.2. Gestational growth Physiology Model**

190 The dynamic physiological parameters for the pregnant mother that changes during the
191 gestational period such as plasma volume, hematocrit percentage, the fetus and the
192 placental growth were accounted for the development of P-PBPK model. The increase
193 in maternal body weight was accounted by considering the dynamic growth of mother's

194 organ and fetus growth into the model. The volumes of liver, kidney, skin, brain, and
 195 gut of mother were calculated by taking constant fractions of the non-pregnant
 196 maternal body weight (Brown et al., 1997) provided in Table A.1. For the rest of the
 197 body compartment for pregnant mother and fetus was calculated by subtracting the
 198 sum of all organs volume from the total maternal and fetus body weight respectively.
 199 Additionally, increased the blood flow to the organs such as kidney, fat and placenta
 200 were considered to calculate the increase in maternal cardiac output (O’Flaherty et al.,
 201 1992; Gentry et al., 2003, 2002). All physiological parameters were considered as a
 202 function of gestational day and the model equations were adapted from different
 203 literature sources (O’Flaherty et al., 1992; Gentry et al., 2003, 2002; Abduljalil et al.,
 204 2012) and are provided in appendix-I.

205 The fetus model was sub compartmentalized into liver, plasma, brain, amniotic fluid
 206 and rest of the body. Fetal body and mother placental volume was modeled by using
 207 equation (1) and equation (2), respectively, described by Gentry et al., (2003). The
 208 quantity of amniotic fluid for the gestational day was calculated by applying polynomial
 209 equation (3), as described by Abduljalil et al., (2012). Fetal blood flow was defined as a
 210 function of fetal blood volume and is adapted from the Clewell et al., (1999). Fetus
 211 plasma blood flow to the individual organs was calculated using equation (5) that
 212 implies multiplication of the fetal cardiac output with a constant fraction of the fetal
 213 blood flows to those organs, which assumed to be same as mother, as described by
 214 Gentry et al., (2003). Blood plasma flow to the rest of body was derived by subtracting
 215 the sum of total blood plasma flow to the organ from the total fetal cardiac output. The
 216 dynamic growth of the fetus volume was calculated during its gestational growth using
 217 equation (1). The fetus growth data provided by Brown et al., (1997) and ICRP, (2002)
 218 were used to calculate the fetus organ weight as a constant fraction of its body weight
 219 which is dynamic parameter described in equation (1). Thus the fetus organ volume
 220 was estimated by multiplying fetal body volume with constant fraction value of the
 221 organs described in equation (4).

222 The fetus, placenta, and amniotic fluid growth kinetics were calculated by applying the
 223 following equations:

$$224 \quad V_{fetus} = (3.779 * \exp(-16.081 * (\exp(-5.67e - 4 * (GD * 24)))) + 3.883 * \exp(-140.178 * (\exp(-7.01e - 4 * (24 * GD)))) \quad \text{eq(1)}$$

$$227 \quad V_{placenta} = 0.85 * (\exp(-9.434 * \exp(-5.23e - 4 * (GD * 24)))) \quad \text{eq(2)}$$

$$229 \quad V_{amniotic\ fluid} = 1.9648 * (GD/7) - 1.2056 * (GD/7)^2 + 0.2064 * (GD/7)^3 - \\ 230 \quad 0.0061 * (GD/7)^4 + 0.00005 * (GD/7)^5$$

231

232

eq(3)

233 Where, V_{fetus} = volume of the fetus in L, GD = gestational day, $V_{placenta}$ = volume
 234 of the placenta in L, and $V_{amniotic\ fluid}$ = volume of the amniotic fluid in mL.

235 The organ volume of the fetus was scaled by using the following general equation:

236 $V_{organ_{fetus}} = F_{organ_{fetus}} * V_{fetus}$ eq(4)

237 Where, $V_{organ_{fetus}}$ = the organ volume in L, $F_{organ_{fetus}}$ = constant fraction of organ
 238 of fetus volume and V_{fetus} = total volume of the fetus

239 The blood flow to the fetus organ was calculated by using the following general
 240 equation:

241 $Q_{organ_{fetus}} = F_{Q_{organ_{mother}}} * Q_{C_{plasma_{fetus}}}$ eq(5)

242 Where, $Q_{organ_{fetus}}$ = the blood flow to organ in L, $F_{Q_{organ_{mother}}}$ = constant fraction
 243 of the cardiac blood flows to the organs in mother, and $Q_{C_{plasma_{fetus}}}$ = fetus cardiac
 244 total blood flow.

245 All the physiological parameters are provided in the annex-A (Table A.1). The dynamic
 246 growth pregnancy physiology equations are taken from previous studies (Gentry et al.,
 247 2003; Abduljalil et al., 2012) summarised in Table 1.

248

249 Table 1. Parameterization of pregnant mother and fetus physiology

Mother Tissue volume	
Liver volume ^b	$V_{Liver} = F_{Liver} * BW_{init}$
Kidney Volume ^b	$V_{Kidney} = F_{kidney} * BW_{init}$
Gut volume ^b	$V_{Gut} = F_{Gut} * BW_{init}$
Brain Volume ^b	$V_{Brain} = F_{Brain} * BW_{init}$
Plasma volume ^c	$V_{Plasma} = (2.50 - 0.0223GA + 0.0042 * GA^2 - 0.00007 * GA^3) * BW$
Initial fat volume ^a	$V_{Fat_{init}} = BW_{init} * F_{fat}$
Fat volume ^a	$V_{Fat} = BW_{init} * (F_{fat} + 0.09 * e^{-12.90995862} * e^{-0.000797 * GD * 24})$
HCT ^c	$HCT = 39.1 - 0.0544 * (GA * 7) - 0.0021 * (GA * 7)^2$
Placenta Volume ^a	$V_{placenta} = .85 * (e^{-9.434 * e^{-5.23E-4 * GD + 24}})$

Increase in Body weight of pregnant women as due to change in fat, placenta, feus and amniotic fluid weight	$BW = BW_{init} + (V_{Fat} - V_{Fat_{init}}) + V_{placenta} + V_{fetus} + V_{Aminiotic\ fluid}$
Fetus tissue volume	
Fetus volume ^a	$V_{fetus} = 3.779 * (e^{-16.08 * e^{-5.67 * e^{-4 * GD * 24}}}) + (e^{-140.78 * e^{-7.01 * e^{-4 * 24 * GD}}})$
Fetal plasma volume ^b	$V_{Plasma_{fetus}} = F_{Plasma_{fet}} * V_{fetus}$
Fetus liver volume ^b	$V_{liver_{fetus}} = F_{liver_{fet}} * V_{fetus}$
Fetus kidney volume ^b	$V_{kidney_{fetus}} = F_{kidney_{fet}} * V_{fetus}$
Fetus brain volume ^b	$V_{brain_{fetus}} = F_{brain_{fet}} * V_{fetus}$
Amniotic fluid volume ^c	$V_{Aminiotic\ fluid} = 0 + 1.9648 * GA - 1.2056 * GA^2 + 0.2064 * GA^3 - 0.0061 * GA^4 + 0.00005 * GA^5$
Fetus rest of body volume	$V_{restbody_{fetus}} = (0.92 * V_{fetus}) - (V_{Plasma_{fetus}} + V_{liver_{fetus}} + V_{kidney_{fetus}} + V_{brain_{fetus}})$
Blood flow to mother tissue (L/h)	
Initial cardiac output for blood ^b	$QC_{Blood_{init}} = QCC * BW_{init}^{(75)}$
Adjust initial cardiac output for plasma flow ^b	$QC_{Plasma_{init}} = QC_{init} * (1 - HCT)$
Plasma flow to liver ^b	$Q_{Liver} = F_{QLiver} * QC_{Plasma_{init}}$
Plasma flow to gut ^b	$Q_{Gut} = F_{QGut} * QC_{Plasma_{init}}$
Initial flow to fat ^b	$Q_{Fat_{init}} = F_{QFat} * QC_{Plasma_{init}}$
Changing flow to the fat ^a	$Q_{Fat} = Q_{Fat_{init}} * \left(\frac{V_{Fat}}{V_{Fat_{init}}} \right)$
Blood flow to placenta ^a	$Q_{Placenta_{blood}} = 58.5 * V_{placenta}$
Plasma flow to placenta	$Q_{Placenta} = Q_{Placenta_{blood}} * (1 - HTC)$
Renal plasma flow ^c	$Q_{Kidney} = 53 + 2.6616 * GA - 0.0389 * GA^2$

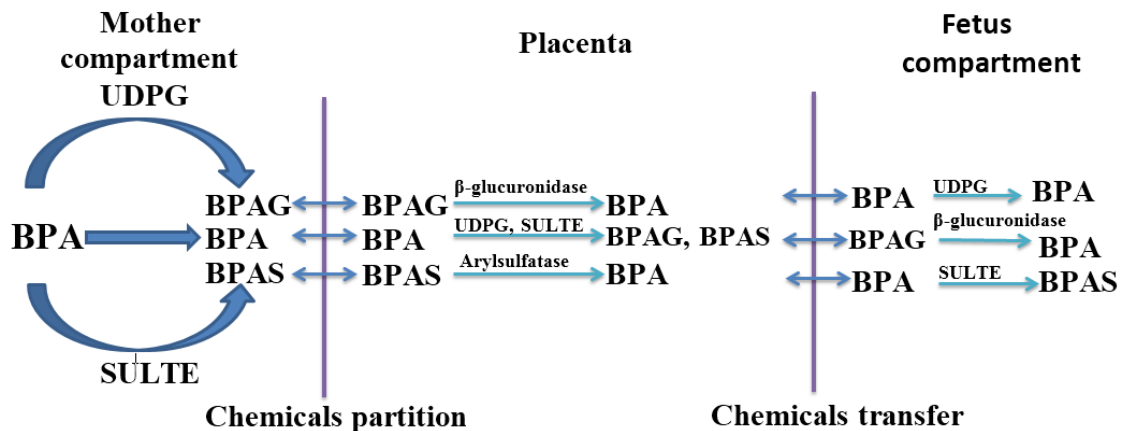
Cardiac output ^b	$QC = QC_{init} + (Q_{Fat} - Q_{(Fat_{init})}) + (Q_{Kidney} - Q_{Kidney_{int}}) + Q_{Placenta}$
Blood flow to fetus (L/h)	
Cardiac output for fetus ^b	$QC_{blood_fetus} = FQ_{fetus} * V_{Plasma_fetus}$
Fetal cardiac output adjusted to plasma ^b	$Q_{plasma_fetus} = QC_{Blood_fetus} * (1 - HCT_{fetus})$
Fetal liver blood flow ^b	$QLiver_fetus = FQLiver * QC_{Plasma_fetus}$
Fetal kidney blood flow ^b	$QKideny_fetus = FQKidney * QC_{Plasma_fetus}$
Fetal brain blood flow ^b	$QBrain_fetus = FQBrain * QC_{Plasma_fetus}$

250 **a** = (Gentry et al., 2002), **b** = standard scaling method for PBPK, **c** = (Abduljalil et al., 2012)

251 GD= Gestational day, GA = Gestational age in week

252 2.3. BPA Pharmacokinetics

253 The conceptual schema has been provided in the Figure 2 showing distribution of BPA
254 and its metabolites in the body.



255

256 Figure 2. The pharmacokinetics of BPA and its conjugates in both mother and fetus.
257 The placental-fetal unit assumes a bidirectional transfer process of BPA and BPA-C
258 describing the distribution of BPA and its metabolites in mother and fetus body.

259

260 In the present P-PBPK model of BPA, physiological changes during pregnancy were
261 included. Metabolism in pregnancy was introduced via scaling of the in-vitro Vmax for
262 glucuronidation and sulfation, considering the pre-pregnancy body weight. The BPA
263 metabolism data for the fetus was scaled using human in-vitro data and fetus
264 microsomal protein content, and, growing fetus liver and body weight. Two metabolic
265 kinetic parameters namely Vmax (maximum rate of reaction) and Km (affinity of the

266 substrate for the enzyme), for mother and fetus, is taken from in-vitro studies and has
267 been scaled to in-vivo. The pharmacokinetic data are provided in the annex-A (Table
268 A.2).

269

270 **2.3.1. Oral uptake and gut metabolism:** Generally, the oral ingestion of BPA
271 through diet is considered as the major route of exposure (WHO, 2010). It is rapidly
272 absorbed through the gut and maximum concentration in the blood achieves at 0.42-1
273 h. Studies have shown that oral bioavailability of BPA is very low, as it passes through
274 first pass metabolism, in the intestine and liver, being completely absorbed from the gut
275 (Völkel et al., 2005, 2002; Mielke and Gundert-Remy, 2012).

276 Both BPA and BPAG uptake from the gut to the system was described by first order
277 reaction, considering gastric emptying delay for BPA arrival to the gut. The oral
278 absorption rate of the BPA was optimized against the Yang et al. (2015) data. The data
279 on uptake of BPAG from the intestine to the liver was taken from the previous study of
280 Yang and Fisher, (2015).

281 Most of the oral administered BPA metabolizes into BPAG by intestinal UDPGT (Mazur
282 et al., 2010; Trdan Lusin et al., 2012). The in-vitro in-vivo extrapolation (IVIVE)
283 approach and saturation metabolism kinetic (eq. 6) were applied for describing BPA
284 glucuronidation in the mother intestine (Cubitt et al., 2009; Yoon et al., 2014). The
285 scaling of in-vitro V_{max} parameter to in-vivo (IVIVE) was done applying equation (7)
286 that used microsomal protein content per gram tissue and weight of tissue per kg body
287 weight. For the scaling of V_{max} , the amount of microsomal protein in the gut of 3mg/g
288 (MPPGG) and the weight of human gut 30g/kg body weight was taken into account
289 (Yang and Fisher, 2015)

290 The metabolism is described by using the following equation:

291

$$292 \frac{dA_{met}}{dt} = \frac{V_{max} * C_{organ} * f_u}{K_m + C_{organ} * f_u} \quad eq(6)$$

293

294 Where, $\frac{dA_{met}}{dt}$ = the amount of metabolism produced with time, V_{max} = the maximum
295 metabolism rate, K_m = the concentration of substrate required to attain 50 percent of
296 its V_{max} , C_{organ} = the concentration of substrate at target metabolism organ, and f_u =
297 fractional unbound.

298 V_{max} was scaled to in-vivo per kg BW from in-vitro cell line studies by using the
299 following method:

$$300 V_{max}(intestine) = (V_{max_{invitro}} * MPPGG * V_{gut}) / BW^{.75} \quad eq(7)$$

301

302 Where, $V_{max_{invitro}}$ = in-vitro value of metabolic capacity in per gram of microsomal
303 protein (intestinal cell line) , $MPPGG$ = microsomal protein per gram of gut , V_{gut} = total
304 gut weight in gram, and BW = whole body weight in kg.

305

306 **2.3.2. Dermal absorption and metabolism:** Recently published papers raised the
307 issue of underestimation of BPA exposure via the dermal route given that BPA
308 presence in materials that frequently comes in contact with the human skin
309 (Biedermann et al., 2010; Lassen et al., 2011; Mendum et al., 2011). In-vitro viable skin
310 culture model experiments showed that the skin has potential to absorb and metabolize
311 BPA into BPAG and BPAS (Kaddar et al., 2008; Zalko et al., 2011a). Recently, Mielke
312 et al., (2011) published internal dosimetry model of BPA compared oral route with 90
313 percent absorption rate, with dermal route considering different reported absorption
314 rates such as 10 (EU, 2003), 13 (Morck et al., 2010), 46 (Zalko et al., 2011b), and 60
315 (Biedermann et al., 2010) and showed importance of the dermal absorption for the
316 estimation of BPA internal exposure level.

317 In the present study, the dermal route of exposure was considered for the development
318 of P-PBPK model. Considering the fact of wide variation of the absorption rate of BPA
319 via skin, highest reported permeability coefficient ($k_{as} = 0.25$ 1/hr), data for the adult
320 model provided by Mielke et al., (2011) was used to develop the P-PBPK model. The
321 following equation (8) was applied for calculating skin absorption:

$$\frac{d}{dt} skin = Q_{skin} * (C_{plasma} * fu - C_{skin} * \frac{fu}{K_{skin_plasma}}) + (C_{app_skin} - c_{skin}/K_{skin_vehicle}) * t_{df} * kas * A/1000$$

324

eq(8)

325 Where, Q_{skin} = the cardiac blood flow to skin, C_{plasma} = the plasma chemical
326 concentration, fu = the fractional unbound, K_{skin_plasma} = the plasma skin partition
327 coefficient, C_{app_skin} = the applied concentration of chemical to the skin surface,
328 C_{skin} = the concentration of chemical in the skin compartment, $K_{skin_vehicle}$ = the
329 vehicle skin partition coefficient, t_{df} = the time delay factor for absorption to reach to
330 plasma, A = skin surface area and k_{as} = the permeability rate constant.

331 **2.3.3. Metabolism in the adult liver:** Phase-II glucuronidation reaction is a major
332 pathway in human for chemicals or drugs detoxification. The resulting conjugates of
333 glucuronic acid to the chemicals increase its hydrophilicity and are generally
334 considered to be pharmacologically inactive (Sperker et al., 1997b). BPA undergoes
335 rapid metabolism to form glucuronidation and sulfation conjugates in the liver by

336 uridine-diphospho-Glucoronide transferase (UDPGTs) and sulfotransferase
337 (SULT)enzyme respectively (Kim et al., 2003; Hanioka et al., 2008, Hanioka et al.,
338 2011). The reported values of Vmax and Km for glucuronidation from different in vitro
339 studies show variability in glucuronidation (Elsby et al., 2001; Kuester and Sipes, 2007;
340 Kurebayashi et al., 2010; Mazur et al., 2010; Trdan Lusin et al., 2012).

341 In the present study, the rate of reaction for both glucuronidation and sulfation for the
342 PBPK model was derived by IVIVE scaling approach. The current hepatic in-vitro cell
343 line data were used for deriving maximum reaction velocity (Coughlin et al., 2012)
344 using equation (9) that accounts microsomal protein value (32mg/g of liver) and liver
345 weight (2.6 percentage of BW). The metabolism was described based on Michaelis-
346 Menten equations using equation (6) and implemented into the current PBPK model.
347 The fraction unbound in the microsomes was not accounted for in the calculation of the
348 in vivo values.

$$349 \quad V_{max}(liver) = (V_{max_{invitro}} * MPPGL * V_{liver})/BW^{.75} \quad eq(9)$$

350

351 Where, $V_{max_{invitro}}$ = in-vitro value of metabolic capacity in per gram of microsomal
352 protein (hepatic cell line), $MPPGL$ = the microsomal protein per gram of Liver, V_{liver} =
353 the total liver weight in gram, and BW =the whole body weight in kg

354 **2.3.4. BPA metabolism in the human fetal liver:** Formation of the glucuronide
355 conjugates involves following steps such as rate of supply of substrate (chemicals to be
356 conjugate), the rate of formation and supply of the co-substrate i.e., glucuronic acid,
357 and the expression and the specific activity of the enzyme responsible for
358 glucuronidation i.e., uridine-diphospho-Glucoronide transferase (UDP-GTs). The
359 concentrations ($\mu\text{mol/Kg}$ wet weight) of UDPGLcUA were 59.4 ± 11.3 (fetal liver), $301 \pm$
360 119 (adult liver), 17.8 ± 1.8 (mid-term placenta) and 17.0 ± 1.7 (near term placenta)
361 (Beach et al., 1978; Cappiello et al., 2000; Coughtrie et al., 1988; Kawade and Onishi,
362 1981). The above data shows that the UDPGLcUA is present in the human fetal liver at
363 a 5-fold lower concentration than in the adult liver. Another study has shown that the
364 activity of UDPGT was null at an early stage of the fetus, showing glucuronidation as a
365 potential limiting factor in the human fetus (Strassburg et al., 2002). The expression of
366 these two isoforms UGT2B15 and 2B7 are detectable in human fetal livers during the
367 second trimester of pregnancy and has been stated to account for 18% of the values
368 calculated in adults (Divakaran et al., 2014).

369 In the present study, the glucuronidation of BPA in the model was considered for the
370 fetus. The scaling of Vmax in the case of the fetus liver has been done before by

371 Gentry et al., (2003). However, Gentry method considers the fixed value of Vmax and
372 uses fetus enzyme activity as a fraction of the adult value for the scaling method. For
373 this study, similar to adult's scaling, the metabolism in the fetus liver was directly scaled
374 from the in vitro hepatocyte data, considering the developmental changes in the fetus.
375 The reported microsomal protein content per gram of fetus liver at the age of 9-22
376 gestational week was 10-16 mg (Pelkonen, 1973) and 26 mg (Pelkonen et al., 1973) in
377 two different studies and for the scaling purpose 26 mg/g liver was taken presumably a
378 realistic value at near term of pregnancy, when fetal metabolic capacity is matured. The
379 liver weight for the fetus was provided as a dynamic parameter, which was scaled by
380 taking constant fraction value of liver from ICRP (2002) data, (provided in the annex
381 Table A.1) and its multiplication with growing fetus body (dynamic equation as a
382 function of the gestational day). The concentration of microsomal fraction content per
383 gram liver was assumed to be constant throughout the gestational day. This approach
384 represents an increase in liver enzyme activity with the increase in the fetus liver and
385 body weight. Thus the Vmax value increases with gestational age. The Vmax,
386 maximum velocity reaction for BPA in the fetal liver was derived by using following
387 equation:

$$388 \quad Vmax_{fetus} = (Vmax_{invitro} * MPPGL_{fetus} * V_{liver_{fetus}}) / BW_{fetus}^{.75} \quad eq(10)$$

389 Where, $Vmax_{fetus}$ = maximum metabolism rate of fetus liver, $Vmax_{invitro}$ = reported
390 in-vitro metabolism rate, $MPPGL_{fetus}$ = microsomal protein per gram of fetus liver, and
391 $V_{liver_{fetus}}$ = liver volume of fetus.

392

393 **2.3.5. Deglucuronidation in fetus compartment:** β -Glucuronidase is an enzyme,
394 which deconjugates the glucuronide conjugate xenobiotics (Sperker et al., 1997a).
395 There is evidence for a significant role of the β -Glucuronidase in the fetus, although the
396 role has not been well understood so far in the fetus kinetic modeling. In the animal
397 fetus development studies, it has been found that deglucuronidation activity is more
398 than glucuronidation at the developmental stage (McCance et al., 1949; Lucier and
399 Sonawane, 1977). In contrast at near term, a fetus glucuronidation activity is higher
400 than deconjugation (Corbel et al., 2015). Domoradzki et al., (2003) studies in the fetus
401 rats at different gestational age showed deconjugation activity of 443 nmol/h/mgMSP at
402 the age of 22 weeks showing the importance of deglucuronidation in the fetus.
403 Moreover, glucuronide conjugate versus free BPA ratio in the placenta and fetus
404 showed that β glucuronidase is present at high concentration in placenta and other
405 various tissues in the fetus (Ginsberg and Rice, 2009).

406 **2.4. Fetoplacental BPA kinetics:** Placenta acts as a barrier against xenobiotics such
407 as chemicals and drugs to protect the fetus from being exposed to them. Morck et al.,
408 (2010), in an ex vivo placental perfusion study showed that BPA can easily cross the
409 human placenta. Further, Borriukwisitsak et al., (2012) reported that due to its
410 lipophilic nature, BPA can easily cross the placental barrier. The finding of free BPA in
411 fetus plasma in human biomonitoring (Schönfelder et al., 2002; Ikezuki et al., 2002;
412 Kuroda et al., 2003; Lee et al., 2008; Zhang et al., 2013), showed evidence of transfer
413 of BPA through the placenta. In contrast, very low level of BPAG in the fetus was found
414 (Muna et al., 2013; Gerona et al., 2014) assuming due to the deglucuronidation in both
415 placenta and fetus liver (Nahar et al., 2013; Gerona et al., 2014). In fact, Nishikawa et
416 al., (2010) uterine perfusion experiments showed that small amount of BPAG is
417 transferred to the fetus across the placenta showing very low bidirectional transfer of
418 BPAG

419 The mother plasma and placenta partition coefficient value for BPA and BPAG were
420 taken from a previous study of Csanády et al. (2002) and Kawamoto et al. (2007)
421 respectively. In this model distribution of sulfation conjugate of BPA (BPAS) to the fetus
422 compartment was not considered due to lack of data in placental transfer. The transfer
423 rate constants for BPAG in this model were taken from the pregnant mice PBPK model
424 and scaled to fetal body weight (Kawamoto et al., 2007), as there is no available
425 human data. Additionally, the glucuronidation of BPA in placenta was described,
426 considering Vmax and Km value from an in-vitro hepatic cell line (Coughlin et al.,
427 2012). The in-vivo Vmax for the placenta was calculated using placenta microsomal
428 content i.e., 11.3 mg/g (McLaughlin et al., 2000), placenta volume and the body weight.
429 The scaling of Vmax for placenta glucuronidation was done using following equations:

$$430 \quad V_{max_{placenta}} = (V_{max_{invitro}} * (MPPGP) * V_{placenta}) / BW^{.75} \quad eq (11)$$

431

432 Where, $V_{placenta}$ is the volume of placenta and it is a dynamic parameter, which
433 depends on the Gestational day can be seen in equation 2. $MPPGP$ is microsomal
434 protein per gram of placenta.

435

436 **2.5. Amniotic fluid BPA kinetics:** The human biomonitoring data had reported the
437 presence of BPA and BPAG concentration in amniotic fluid. The increase in free BPA
438 concentration with the increase in the gestational period was observed, as from second
439 trimester to the third trimester (Edlow et al., 2012). Ikezuki et al., (2002) reported the
440 five-fold higher concentration of free BPA at an early stage of pregnancy in comparison
441 to the late week of gestational. This phenomenon might be due to the low metabolic
442 capacity of fetus organ as well as the low volume of amniotic fluid at an early stage of

443 pregnancy. Further, the activity of beta-glucuronidase measured in amniotic fluid at
444 early stage found to be higher than the later week of gestation. Whereas,
445 glucuronidase activity is found to be higher in the later week of gestation (Matysek,
446 1980; Fetus et al., 1993). The above finding of increased activity in glucuronidase at an
447 early stage of pregnancy could be some of the possible reasons for the increased level
448 of free BPA at the early gestational age.

449 **2.6. Partition coefficient for pregnant mother and fetus organs**

450 The partition coefficient (PC) for liver, fat, brain, and skin were taken from the study
451 done by Fisher et al., (2011). The placental and kidney partition coefficient for BPA
452 were taken from Csanády et al., (2002) and the BPAS was not distributed to fetus
453 tissues. However, to measure BPAG concentration in the fetus plasma, BPAG was
454 distributed to maternal placenta using placenta partition coefficient taken from the
455 previous mice study (Kawamoto et al., 2007). For other fetus compartments, partition
456 coefficients were kept similar to as mother's organs partition coefficients. The partition
457 coefficients used in the P-PBPK model are provided in the annex (Table A.2).

458 **2.7. Pregnancy cohort studies**

459 For this study, we have used 5 different pregnancy cohort studies that measure the
460 BPA concentration in different matrices. Subject characteristics are provided in the Table
461 A.3, which was used as an input variable for the case specific scenario. Summary of
462 the biomonitoring data is provided in the annex (Table A.4). Schönfelder et al. (2002)
463 studies included 37 samples of both mother and fetus plasma (umbilical cord) between
464 the gestational age of 32 to 41 week. Pregnant women of age ranging from 22-44
465 years old were recruited from Berlin and samples were collected at Benjamin Franklin
466 Medical Center. In another study by Aris (2014), which included 61 pregnant women
467 recruited from the eastern township of Canada at delivery time and both mother plasma
468 and fetal cord blood BPA was analyzed.

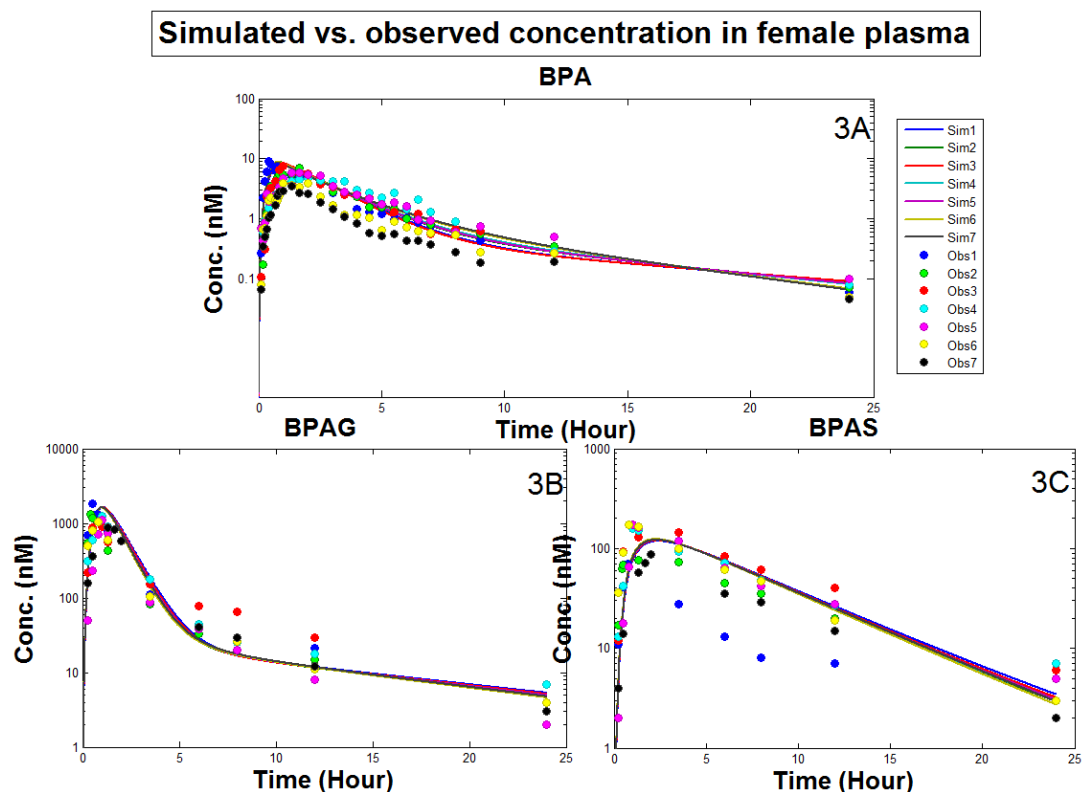
469 Zhang et al. (2011) study included each 21 samples of human placental and fetal liver
470 at the gestational age of 12.3–20 weeks and 11.3-22, respectively. Samples
471 were obtained after elective pregnancy termination during 1998–2006 in the Greater
472 Montreal area of Quebec. In addition, Cao et al. (2012) study included a large number
473 of placenta and liver samples from the same population i.e. 128 and 28, respectively. In
474 addition, Schönfelder et al. (2002) also studied placenta BPA concentration at the
475 delivery time. Ikezuki et al. (2002) studied includes Japan population of each 37
476 women with an early and late pregnancy, where 37 maternal (late pregnancy) and 32
477 umbilical cord blood samples were collected at full-term delivery. In addition, 32 and 38

478 amniotic fluids samples were collected at 15–18 weeks gestation (early pregnancy) and
479 at full-term (late pregnancy), respectively.

480 3. Results

481 3.1. Simulation and Validation of adult human PBPK model

482 Validation of the developed adult PBPK model was performed by comparing the model
483 predictions with plasma data obtained from the human study by Thayer et al., (2015) in
484 which volunteers were orally administered 100 µg/kg BW dose of deuterated BPA.
485 These predictions were performed by taking into account only female volunteers, and
486 their individual BMI and body weight. The exposure dose was normalized according to
487 body weight and the fat content of individual volunteers was calculated based on body
488 weight and BMI of the respective subject. Out of 14 subjects (male and female), only 7
489 female subjects were considered from Thayer’s study and simulated time-plasma BPA
490 data profile were validated against their observed data. The total duration of simulation
491 was 24 h. Figures 3A, 3B and 3C depict the concentration–time profiles after single oral
492 dosing of adult females (n = 7) for BPA (d6-BPA), and observations made by Thayer et
493 al. (2015).



494

495 Figure 3. Concentrations–time profiles after oral dosing of adult females (n = 7) with
496 100 µg/kg of deuterated BPA (d6-BPA) (Thayer et al., 2015). A) Simulated individual
497 (solid color lines) and observed individual plasma (dot points) d6-BPA concentrations;
498 B) Simulated individual (solid color lines) and observed individual plasma (dot points)
499 d6-BPAG concentrations; C) Simulated individual (solid color lines) and observed
500 individual plasma (dot points) d6-BPAS concentrations. Simulations of individual
501 patients were performed using individual body weights and their fat content while
502 keeping other model parameters constant.

503 **3.2. Simulation and evaluation of P-PBPK Model**

504 Most of the reported human biomonitoring data for the fetus is for BPA and generally,
505 BPAG and BPAS studies are under-reported (Ikezuki et al., 2002; Schönfelder et al.,
506 2002; Kuroda et al., 2003; Lee et al., 2008; Zhang et al., 2013). Development of the
507 present model includes BPAG and BPAS conjugates in the mother, whereas in the
508 case of the fetus only BPAG has been accounted, which is the major metabolite
509 produced in the mother. For this study, the distribution of BPA and BPAG from mother
510 plasma to the placenta is described via partition coefficient. Following that transfer of
511 both BPA and BPAG across the placenta was described as simple diffusion process
512 between the placenta and fetus plasma. Human Biomonitoring data showed the
513 presence of higher concentration of free BPA in the amniotic fluid in early pregnancy
514 than compared to late pregnancy (Ikezuki et al., 2002; Edlow et al., 2012). The reason
515 behind this difference could be the higher beta-glucuronidase activity in early and mid-
516 gestational periods (Matysek, 1980). However, in the later week of gestation, as the
517 fetus liver develops and matures that might increase the liver glucuronidation activity.
518 Though there is a lack of glucuronidase data specific to the fetus deconjugation,
519 presuming deconjugation process as an important toxicokinetic process, in the present
520 P-PBPK model it was taken into account for the fetus compartment. The assumption
521 has made that deconjugation of the BPAG to BPA was based on first-order rate
522 transfer constant. The half-life of the chemicals is used to establish the rate of
523 deconjugation estimated to be 0.35 hr^{-1} ($k = 0.693/t_{1/2}$). The same value is used in the
524 case of both placental and fetus deconjugation for simplification. A similar approach
525 has been used in the previous study (Lorber et al., 2010) for transfer of one metabolite
526 to another, but it should be considered as worst case scenario and it shows clearly
527 there is a need for proper studies to parameterise this process. This steps would
528 results in increased level of free BPA in the fetus plasma. To maintain the cyclic
529 deconjugation and conjugation reaction into the model, the available free BPA

530 undergoes simultaneously for glucuronidation into the liver following distribution to the
531 liver compartment to mimic the real biological phenomena.

532 The lack of validation of a model for the estimated exposure (for respective cohort)
533 against biomonitoring data for cohorts via PBPK model has been observed in the
534 previous study by Mielke and Gundert-Remy, (2009). Additionally, finding of
535 differences in the biomonitoring data for free BPA concentration within the cohort and
536 in between cohorts is observed in different biomonitoring studies (Ikezuki et al., 2002;
537 Schönfelder et al., 2002; Kuroda et al., 2003; Lee et al., 2008; Zhang et al., 2013).
538 Several possible reasons can be put forward to explain this inconsistency among which
539 underestimation of exposure levels and not considering other routes of exposure than
540 oral has been questioned by researchers (Mielke et al., 2011). The timing of sampling
541 is one of the major concern that has not been accounted in biomonitoring data, which
542 can be another source of variability in biomonitoring data due to fast absorption and
543 elimination of BPA that never reach steady state concentration even with multiple
544 doses. In targeted human kinetic studies (Völkel et al., 2002; Thayer et al., 2015), the
545 observation of C_{max} (maximum concentration) and elimination half-life within 1-3 hours
546 of BPA exposure shows how crucial is the time of sampling. However variability due to
547 the analytical method, contamination, source and route of exposure (EFSA, 2015;
548 Longnecker et al., 2013; Ye et al., 2013), and importantly metabolic variation among
549 population cannot be ruled out (Partosch et al., 2013; Nachman et al., 2014), which is
550 beyond the scope of this manuscript.

551 Another complexity with the prediction of concentration for such chemicals might be
552 due to their narrow time interval between the C_{max} (the highest concentration) and
553 C_{min} (minimum concentration after exposure of chemical during 24 hr or before
554 subsequent exposure of chemical) rising a question on observed biomonitoring data is
555 because of high/low exposure or because of the schedule of sampling. Therefore
556 evaluation of the developed model has two possibilities first; either by changing
557 exposure dose for each biomonitoring study, second; by using two extreme exposure
558 scenarios (low-high). In this study, it was assumed that sampled biomonitoring data
559 can be from any point of the time-concentration profile and the exposure dose was
560 estimated for the observed high and low mother plasma concentration. This
561 assumption seems conservative, but for the current scenario, this might be the best
562 solution, instead of estimating exposure for each biomonitoring study. Exposure dose
563 for the biomonitoring data was estimated by taking the reference of a previous study
564 (Mielke et al., 2011). In the present study, the oral exposure was divided into three

565 equal doses keeping dermal exposure as a single dose. Exposure dose for both the
566 oral and dermal was estimated that matches the observed highest and lowest mother
567 plasma concentration in different biomonitoring studies. This was done by simply
568 applying trial and error method, a similar method was used before for other
569 environment chemicals (Loccisano et al., 2013). Then the estimated dose was used for
570 the simulation of a model that predicts the fetus plasma and organs concentrations at
571 the different gestational period.

572 We have selected 5 different pregnancy cohort studies that measure the BPA
573 concentration in different matrices. Two scenarios were selected for the simulation of
574 PBPK model: one with the observed high mother plasma concentration population
575 (Schönfelder et al., 2002), in turn dose of 44µg/kg/BW thrice in a day (TID) oral dose
576 and 20µg/kg/BW single dermal exposure and other with the observed low mother
577 plasma concentration (Ikezuki et al., 2002), in turn dose estimated to be 20µg/kg/BW
578 (TID) oral dose and 9µg/kg/BW single dermal exposure.

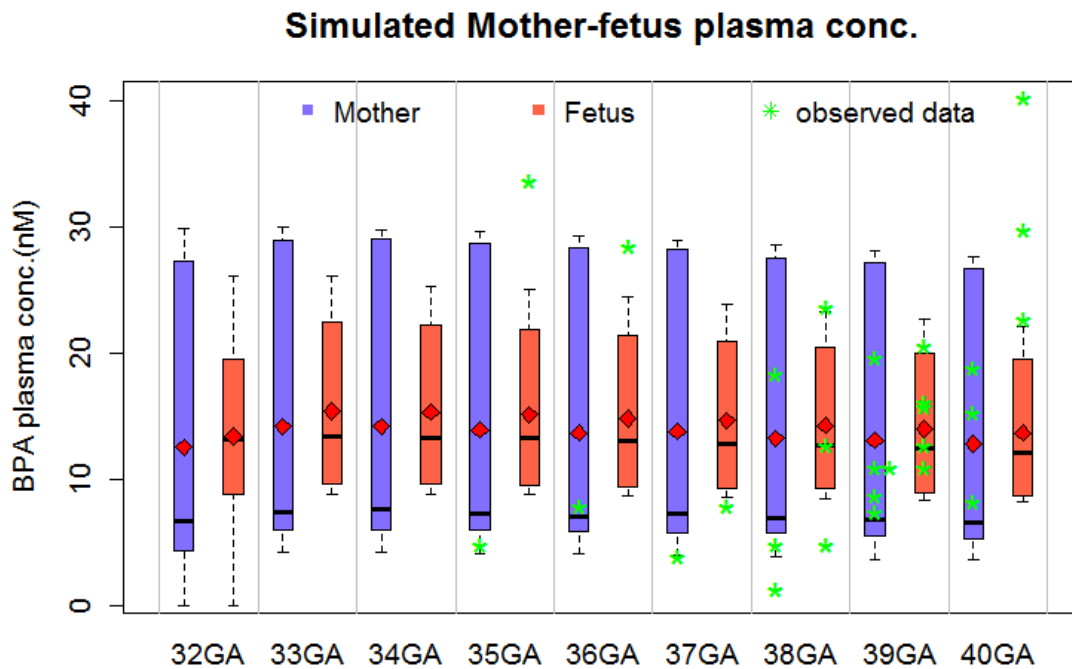
579 Since the BPA has a very short half-life, even with well-distributed dosing schedule, the
580 BPA plasma concentration shows sharp elimination curve profile and did not arrive at
581 the steady state; a similar observation has been made by Mielke et al. (2011). In order
582 to cover all the simulated data points considering essential for comparisons against the
583 observed biomonitoring data points, which could be either result of random samples at
584 any point of time not knowing the exact exposure time or exposure variability in sample
585 subjects (VandeVoort et al., 2016). The model output data were summarized into
586 boxplot for each gestational week, which included the range of value from higher to
587 lower concentration.

588 The simulation was done for different matrices and results were presented in different
589 Figures, a number from 4 to 7. Figure 4 & 5 shows the simulated results for mother and
590 fetus BPA plasma concentration for the selected high and low dose exposure scenario
591 respectively. Figure 6 shows the simulation results for the BPA concentration in liver
592 and placenta during the mid-gestational week and the results were compared with the
593 biomonitoring data obtained from Zhang et al. (2011) study. Figure 7 shows the BPA
594 concentration in amniotic fluid. The amniotic fluid concentration of BPA by Ikezuki et al.
595 (2002) was monitored at two stages, early and full term pregnancy. The low dose
596 scenario was simulated for the Ikezuki et al. (2002) data on the concentration of BPA in
597 mother and fetus plasma (Figure 5) and amniotic fluid concentration (Figure 7). The
598 Figure 7 shows the predicted BPA concentration in amniotic fluid is well matched with
599 the observed concentration. Moreover, the observed mother and fetus plasma

600 concentration (mean \pm SD) by Ikezuki et al. (2002) is within the range of simulated low
601 dose exposure scenario (Figure 8).

602 Figure 8 shows the predicted mean \pm SD for the high and low dose scenario vs.
603 observed mean \pm SD of different cohort studies for the period during 32-40 week of
604 gestation. Most of the observed mean concentration was covered by a simulated
605 scenario in case of mother plasma given the large range between Cmax and Cmin.
606 However, in the case of the fetus some observed mean values were not in the range,
607 which could be due to the various factors such as; variability in the gender of fetus
608 previously reported as significant, metabolic variability due to polymorphism (not
609 considered in this study) and process of deglucuronidation, which need proper in-vitro
610 investigation for parameterization.

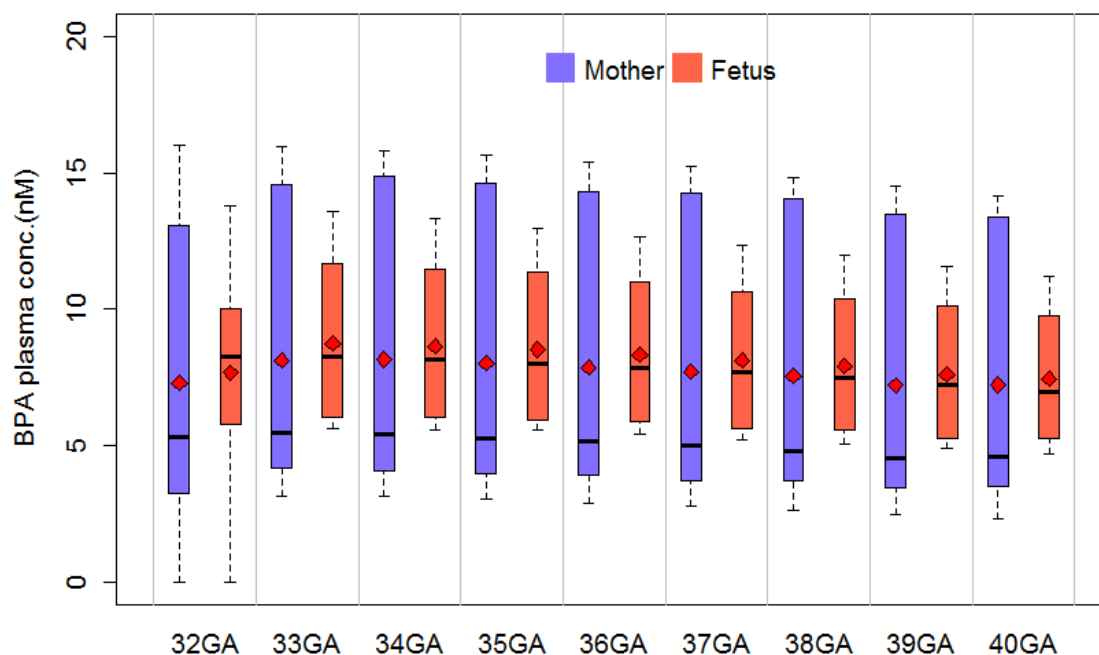
611



612 Figure 4. Observed vs predicted mother plasma and fetus plasma of volunteer
613 participated in Schönfelder et al. (2002) study for 32 to 41week of GA; box plot
614 containing mean (red diamond), median (horizontal line of boxplot), highest (upper bar
615 of boxplot), lowest (lower bar of boxplot) value and observed value marked as green
616 star.

617

Simulated Mother-fetus plasma conc.



618

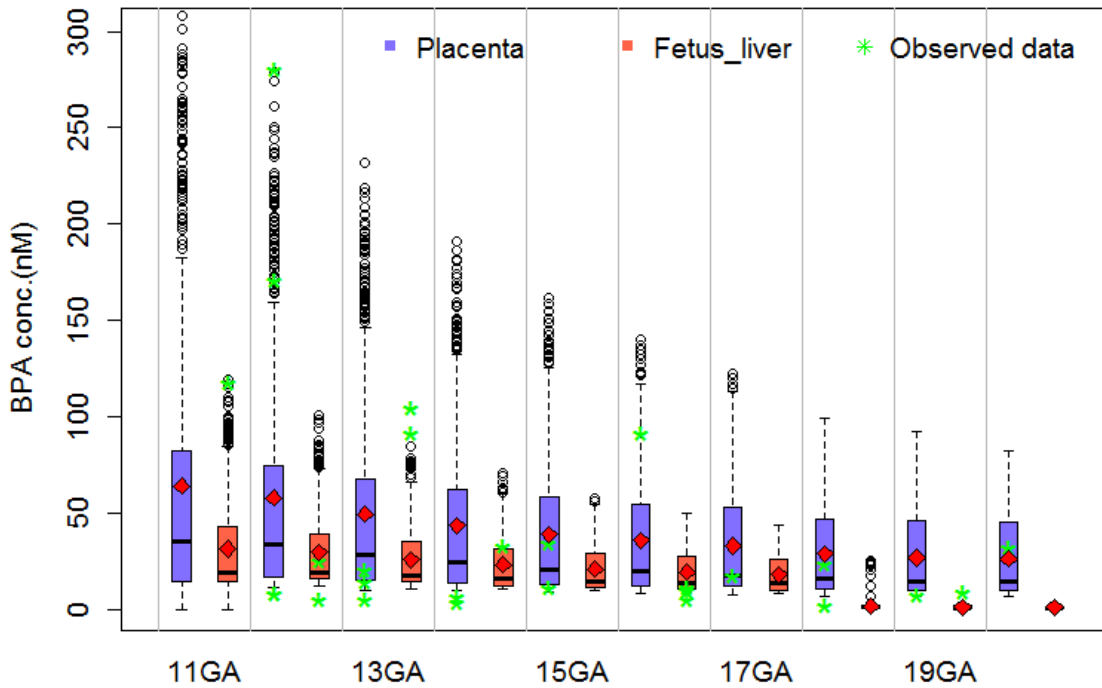
619 Figure 5. Predicted mother plasma and fetus plasma for low dose scenario, estimated
620 from the Ikezuki et al. (2002) mother plasma concentration, for 32 to 41 week of GA;
621 box plot containing mean (red diamond), median (horizontal line of boxplot), highest
622 (upper bar of boxplot), and lowest (lower bar of boxplot) value.

623

624

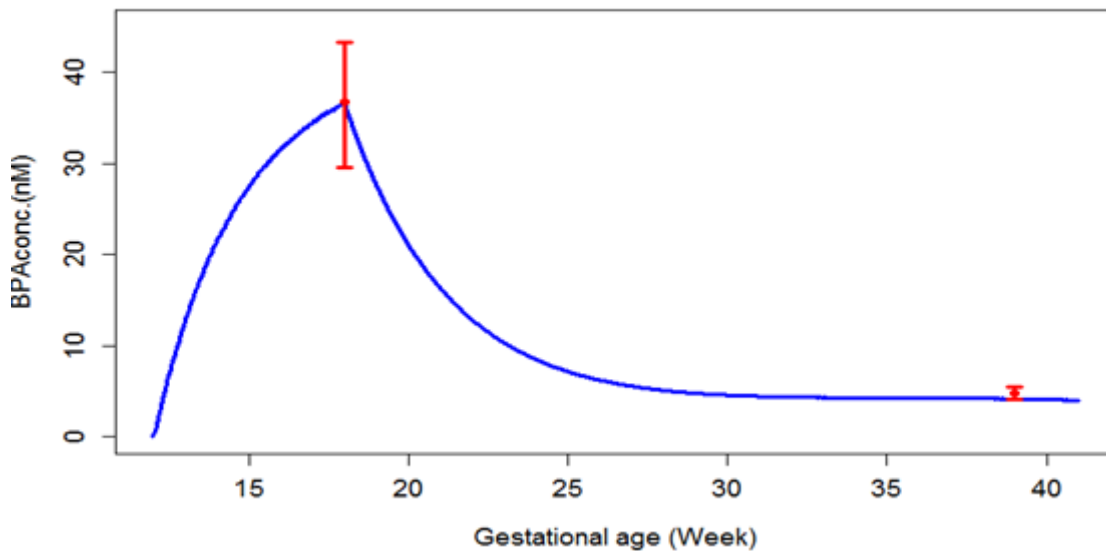
625

Simulated Placenta-fetus liver BPA conc.

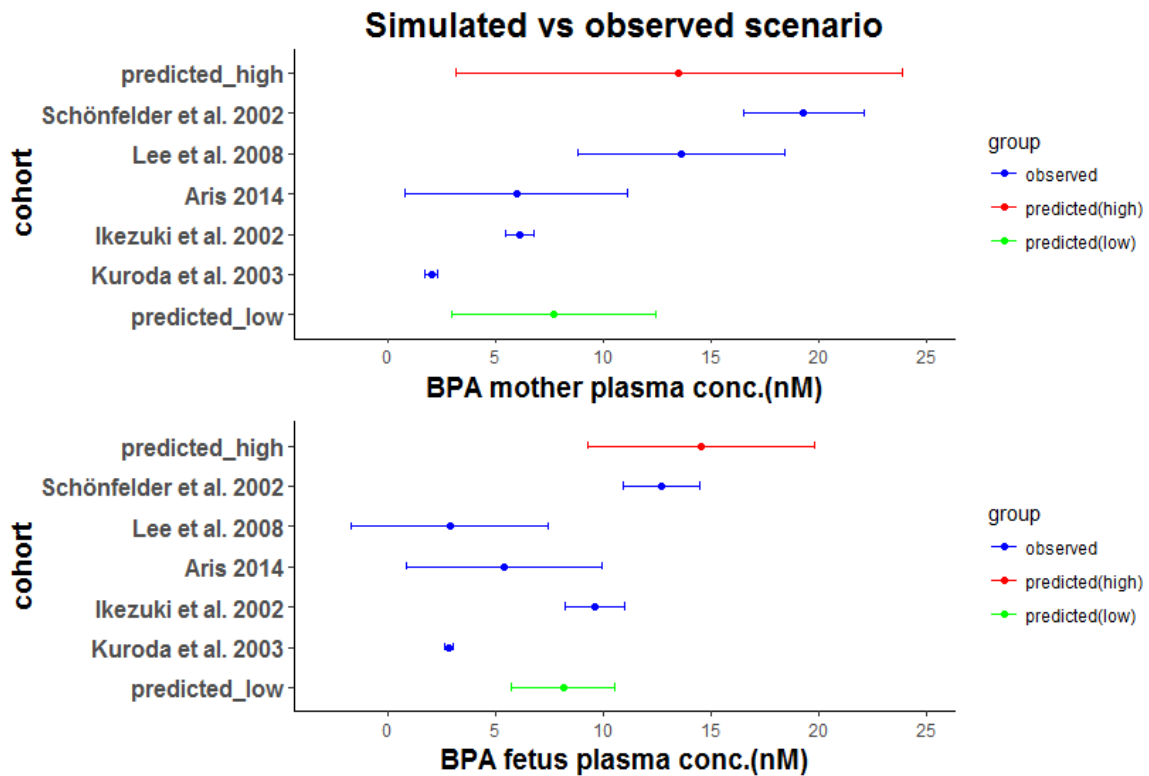


626 Figure 6. Observed vs predicted placenta and fetal liver for higher exposure scenario
 627 for 11 to 22 week of GA; box plot containing mean (red diamond), median (horizontal
 628 line of boxplot), highest (upper bar of boxplot), lowest (lower bar of boxplot) and
 629 observed value (Zhang et al., 2011) marked as green star.

Simulated vs observed BPA conc.in amniotic fluid



630
 631 Figure 7. Simulated low dose exposure scenario for amniotic BPA concentration
 632 starting from early mid-gestational to late gestational period (blue line curve) vs.
 633 observed (mean \pm SD) concentration in Ikezuki et al. (2002) studied during 15-18 and
 634 32-40 weeks of pregnancy (red error bar).



635

636 Figure 8. Simulated mean \pm SD of BPA for two exposure scenario (high and low dose)
 637 for the period of 32-40 GA and the observed mean \pm SD of BPA in different studies for
 638 both mother and fetus BPA plasma concentration.

639 **4. Discussions**

640 The present study involved development and validation of the adult PBPK model and
 641 then an extension of this model to the pregnant mother to predict the toxicokinetic
 642 profile of BPA for both mother and fetus organs. Following the same parameterization
 643 of the previously developed model (Yang et al., 2015), in the present study, it was
 644 observed that results under predicts the free BPA and BPAS in plasma serum. The
 645 reason behind this could be the low absorption rate constant for free BPA, which leads
 646 to higher concentration available in the gut for the metabolism. The present adult model
 647 was slightly modified optimizing absorption rate constant and then the model was
 648 validated against the Thayer et al., (2015) human experimental data. For the validation
 649 of the adult model, only female subjects were taken into consideration and the
 650 simulation for the individual subjects was done considering their physiological
 651 parameters such as body weight and body mass index. The adult pharmacokinetic
 652 results have shown that BPA has very fast absorption and elimination process
 653 (Schönfelder et al., 2002) as it undergoes first pass metabolism and rapidly converted
 654 into more polar compounds (glucuronide conjugates). Due to high metabolic activity for

655 BPA, even higher or multiple doses has very less effect on time-concentration curve
656 characteristic. However, variability in the BPA plasma concentration with respect to the
657 time-concentration curve is much higher than inter-individual variation among subjects,
658 showed plasma concentration is not only sensitive to dose but to time as well. The
659 sudden drop in BPA concentration at peak is due to its higher metabolism rate, making
660 a very sharp curve, which can be considered as benchmark characteristics of BPA.
661 Even within a small fraction of the time, a large difference in BPA concentration was
662 observed in this study. There were no significant changes in BPA plasma concentration
663 observed among subjects, even individual fat content, calculated from body weight and
664 BMI, has very little or no impact on plasma concentration. Although, some study has
665 shown the genetic and gender variability in metabolism among the population (Hanioka
666 et al., 2011). It has been reported that the concentration of BPA varies among different
667 population cohorts such as male and female, pregnant and non-pregnant, adult,
668 neonates, and children (Kim et al., 2003; Calafat et al., 2005; Vandenberg et al., 2010;
669 Zhang et al., 2013; Aris, 2014). Polymorphism has been found to be one of the
670 important factors in metabolic variability (Trdan Lusin et al., 2012). However, there are
671 very few data available on functional polymorphism among the population causing
672 metabolic differences in BPA metabolism. (Hanioka et al., 2011). In the present study,
673 polymorphism variability has not been accounted, however, it cannot be ruled out.
674 Further, the variation in biomonitoring data shows the need for considering different
675 physiological states into the PBPK models. Some specific physiological parameter
676 such as body weight, height, and dynamic physiological changes in the specific
677 population such as pregnancy and fetus were accounted to capture variability. A
678 number of P-PBPK models have been developed for various environmental chemicals
679 in the past for the risk assessment application(O'Flaherty et al., 1992; Gentry et al.,
680 2003, 2002; Loccisano et al., 2013) . Similar approach has been taken for the current
681 P-PBPK model. However, in the current model approach, the model has included
682 detailed chemical metabolism concept in both mother and fetus considering their
683 dynamic growth parameters in order to mimic the real physiological process during
684 gestational period.

685 The observed concentration in different cohorts during pregnancy was used for model
686 evaluation. For instance, maternal blood concentration during pregnancy or at the
687 delivery time was used for exposure estimation accounting both dermal and oral
688 exposure. In the development of P-PBPK model, pregnancy growth dynamic equations
689 were implemented into the model that mimics the physiology of pregnant mother, and
690 the inclusion of the fetus compartment and its communication with the mother was

691 done via placenta blood flow. The metabolism of the BPA in placenta and fetus liver is
692 found to be key parameters for the understanding of fetal exposure to parent BPA. The
693 human hepatocyte in-vitro data was scaled to calculate the fetus liver metabolic
694 activity. For the scaling of Vmax, the reported fetus microsomal protein content was
695 used in place of adult microsomal content. The deglucuronidation process for the fetus
696 liver and amniotic fluid was applied into plasma compartment for the simplification of
697 the model. The P-PBPK model predictions were compared with different sets of the
698 BPA biomonitoring data available in the literature. Simulation-matched study designs
699 were used based on information in the original studies.

700 In order to predict the BPA concentration in fetus plasma for various population studies,
701 observed maternal BPA plasma concentration during pregnancy was used for
702 exposure estimation accounting both dermal and oral exposure. The predicted
703 exposure concentrations for two scenarios (high and low mother plasma concentration
704 considering Schönfelder et al., (2002) and Ikezuki et al. (2002) studies respectively),
705 were chosen and seems to be significantly higher than the generally estimated
706 exposure. A similar observation about predicted and observed concentrations of these
707 two references (Schönfelder et al., (2002) and Ikezuki et al. (2002)) were made in
708 previous studies (Mielke and Gundert-Remy, 2009; Mielke and Gundert-Remy, 2012).
709 The exposure scenarios used in this study are: high dose scenario with 44µg/kg/BW
710 thrice in a day (TID) oral dose and 20µg/kg/BW single dermal exposure and, low dose
711 scenario with 20µg/kg/BW (TID) thrice in a day (TID) oral dose and 9µg/kg/BW single
712 dermal exposure. A similar exposure dose was previously estimated by Mielke et al.,
713 (2011). However, in this study, the estimated dose is lower, given the fact that single
714 oral dose was equally divided into three doses and lag time for dermal dose was
715 included. The simulated results for mother and fetus plasma concentration for two
716 exposure scenario showing median, mean, high and low value for each gestational
717 week were presented in Figure 4 and 5. Most of the biomonitoring observed data are
718 within the simulated results represented in Figure 8. Limited data availability for each
719 gestational week is one of the limitations of the model validation. However, in some
720 cases, fetus plasma of BPA was much higher (Figure 4), which might be explained by
721 gender difference observed previously (Schönfelder et al., 2002), which was not
722 included in the present model. Considering the mean value for each simulated week
723 shown in Figure 4 and 5, fetus BPA mean concentration value is higher than the BPA
724 in mother plasma, which could be explained by the fact that the elimination process in
725 the fetus is not so effective and solely depends on diffusion of chemical back to mother
726 plasma via placenta or to amniotic fluid. Additionally, the model predicted the Cmax

727 and C_{min} relatively higher value for the mother plasma than the fetus plasma
728 concentration.

729 Detailed biomonitoring sample of liver and placenta during 11 to 20 weeks of
730 gestational has been reported (Zhang et al., 2011). It was observed that after the 17th
731 week of gestational, free BPA concentration starts to decrease and appearance of
732 BPAG in the liver, showing the development of the metabolic capacity of the fetus at
733 this stage. To mimic this condition, metabolic activity in fetus liver and placenta was
734 introduced at 17th gestational week. The simulated results for both fetus liver and
735 placenta during mid-gestational were compared with the biomonitoring study of Zhang
736 et al. (2011) (Figure 6). However, some observed data points were below the range of
737 predicted value. An increase in metabolic capacity was observed with the increase in
738 liver weight during the gestational development, which could explain the result of
739 decreasing free BPA concentration.

740 The recent biomonitoring data by Aris, (2014) showed that BPA exposure to the fetus
741 during the mid- gestational is very high ranging from LOD to 229 nM. This
742 biomonitoring data shows that mid-gestational is a very critical window of exposure to
743 the fetus. The developed P-PBPK model has also shown the higher BPA value during
744 mid-gestational weeks compared to near term or at delivery. The reason of relatively
745 higher exposure could be the fetus volume, which is very less at mid-gestational, and
746 also the metabolic capacity, which is presumably active after the 18th week of
747 gestational.

748 The pharmacokinetic differences for the fetus seem to be very dramatic as fetus
749 metabolic capacity and organ physiology system are relatively immature at an early
750 stage of fetal development. The faster chemical metabolism and elimination of the BPA
751 by the maternal system ameliorate BPA kinetics in the fetus to a great degree.
752 However, evidence of finding higher free BPA (Ikezuki et al., 2002; Schönfelder et al.,
753 2002; Aris, 2014) in cord blood as compared to maternal blood in various populations
754 indicates higher fetal exposure and sensitivity to BPA due to pharmacokinetic factors.

755 The simulation of the model for BPA concentration in amniotic fluid during mid-
756 gestation (Figure 7) to near term showed the increasing concentration of the BPA with
757 an increase in the gestational period. The BPA concentration increased until mid-
758 gestational and then slowly started to decrease reaching to almost one and a half fold
759 less than the observed mother plasma concentration. The predicted results are in
760 agreement with observed data of Ikezuki et al., (2002), and have a linear relation with
761 gestational time (less fluctuation in BPA concentration) suggesting amniotic fluid BPA

762 concentration as a good biomarker for identifying the critical window of exposure to the
763 fetus. The prediction of the concentration of free BPA in amniotic fluid was slightly less
764 than reported biomonitoring data observed in late gestational. This could be due to the
765 prediction of slightly high amniotic fluid volume than normally observed in the late
766 gestational period. Factors such as local deconjugation in placenta, the lipophilicity of
767 chemical, relatively higher deconjugation than conjugation in the fetal compartment can
768 affect the propensity for chemicals to reach a higher concentration in the fetal
769 compartment (Nachman et al., 2014).

770 The developed P-PBPK model is in concordance with biomonitoring data and showed
771 that BPA readily transferred to fetal serum and amniotic fluid after mother's exposure.
772 Even, fast metabolism and rapid excretion of BPA and BPA-C are unable to prevent
773 the BPA fetal exposure. The transfer rates of BPA from the placenta to the fetal
774 compartment varied considerably. Deconjugation in placenta and fetus body is of major
775 concern at early fetal life, where metabolism capacity is low, causing an increased level
776 of unconjugated BPA in the fetus. Importantly, free BPA in the fetal compartment are
777 more in steady state and persists even as the maternal level of BPA declines. The
778 consideration of mechanistic approach such as dynamic growth parameters and their
779 governing equations, and model structure could be useful for the development of P-
780 PBPK model for different chemicals.

781 **5. Conclusion**

782 The present study proposed and prospectively developed a P-PBPK model for BPA
783 that describes and predicts the fetus blood and tissues concentrations time profiles
784 based on the mother's exposure scenario. Detail metabolic toxicokinetics in mother and
785 fetus was reviewed and included in the proposed model. Glucuronidation and
786 deglucuronidation in both mother and fetus liver and placenta are found to be an
787 important mechanism that alters BPA toxicokinetic profile. For the development of the
788 model, a two-stage approach was employed: first the development and validation of the
789 adult PBPK model against the kinetic data from control human experimental study and
790 second extension of the adult model to the P-PBPK model and further evaluation with
791 the available BPA biomonitoring cohort studies. The prediction of higher concentration
792 of BPA during the mid-gestational period in the amniotic fluid, placenta, and the fetus
793 liver are in accordance with biomonitoring data, indicating mid-gestational period might
794 be the critical window of exposure for the fetus. Due to the fast absorption and short
795 half-life of BPA, it is showing extreme concentration variability with respect to time,
796 which makes the task of prediction of biomonitoring data very difficult. This study

797 considered two extreme dose scenarios (min-max) for the simulation and in turn
798 plotting of simulated data under the box plot to capture all the data set that allows
799 comparing with biomonitoring data. It has an assumption that biomonitoring sample can
800 be from any time point. However, in order to address the issue of temporal variation of
801 short life chemical, there is a need to have very control case studies dealing with the
802 timing of exposure (food intake) and schedule of sampling. In this study, there are
803 several data gaps identified, which need to be addressed to improve the model. For
804 example, kinetics of BPA glucuronidation/sulfation and deglucuronidation/desulfation at
805 the fetus level, and placental BPA conjugation and deconjugation, and metabolic
806 variation due to functional polymorphism among the different population, are some of
807 the major concern.

808 **Acknowledgement**

809 Preparation of this manuscript was supported in part for European Union's projects,
810 HEALS (Health and Environment-wide Associations via Large population Surveys) by
811 the FP7 Programme under grant agreement no. 603946 and EuroMix (European Test
812 and Risk Assessment Strategies for Mixtures) by the Horizon 2020 Framework
813 Programme under grant agreement no. 633172. Raju Prasad Sharma has received a
814 doctoral fellowship from Universitat Rovira i Virgili under Martí-Franquès Research
815 Grants Programme. This publication reflects only the authors' views. The Community
816 and other funding organizations are not liable for any use made of the information
817 contained therein.

818 **References**

- 819 Abduljalil, K., Furness, P., Johnson, T.N., Rostami-Hodjegan, A., Soltani, H., 2012.
820 Anatomical, Physiological and Metabolic Changes with Gestational Age during
821 Normal Pregnancy. *Clin. Pharmacokinet.* 51, 365–396. doi:10.2165/11597440-
822 000000000-00000
- 823 Aris, A., 2014. Estimation of bisphenol A (BPA) concentrations in pregnant women,
824 fetuses and nonpregnant women in Eastern Townships of Canada. *Reprod.*
825 *Toxicol.* 45, 8–13. doi:10.1016/j.reprotox.2013.12.006
- 826 Beach, L., Adminisrration, V., Hospital, L.K., Angeles, L., 1978. Reduced Hepatic
827 Bilirubin Uridine Diphosphate Glucuronyl Transferase and Uridine Diphosphate
828 Glucose Dehydrogenase Activity in the Human Fetus. *Pediat. Res.* 12, 838–840.
- 829 Biedermann, S., Tschudin, P., Grob, K., 2010. Transfer of bisphenol A from thermal
830 printer paper to the skin. *Anal. Bioanal. Chem.* 398, 571–576.
831 doi:10.1007/s00216-010-3936-9
- 832 Borriukwisitsak, S., Keenan, H.E., Gauchotte-lindsay, C., 2012. Effects of Salinity , pH
833 and Temperature on the Octanol-Water Partition Coefficient of Bisphenol A. *Int. J.*
834 *Environ. Sci. Dev.* 3, 460–464.
- 835 Brown, R.P., Delp, M.D., Lindstedt, S.L., Rhomberg, L.R., Beliles, R.P., 1997.
836 Physiological parameter values for physiologically based pharmacokinetic models.
837 *Toxicol. Ind. Health* 13, 407–484.
- 838 Cabaton, N.J., Canlet, C., Wadia, P.R., Tremblay-Franco, M., Gautier, R., Molina, J.,
839 Sonnenschein, C., Cravedi, J.P., Rubin, B.S., Soto, A.M., Zalko, D., 2013. Effects
840 of low doses of bisphenol a on the metabolome of perinatally exposed CD-1 mice.
841 *Environ. Health Perspect.* 121, 586–593. doi:10.1289/ehp.1205588
- 842 Calafat, A.M., Kuklennyik, Z., Reidy, J.A., Caudill, S.P., Ekong, J., Needham, L.L., 2005.
843 Urinary concentrations of bisphenol A and 4-Nonylphenol in a human reference
844 population. *Environ. Health Perspect.* 113, 391–395. doi:10.1289/ehp.7534
- 845 Cao, X.L., Zhang, J., Goodyer, C.G., Hayward, S., Cooke, G.M., Curran, I.H.A., 2012.
846 Bisphenol A in human placental and fetal liver tissues collected from Greater
847 Montreal area (Quebec) during 1998-2008. *Chemosphere* 89, 505–511.
848 doi:10.1016/j.chemosphere.2012.05.003

849 Cappiello, M., Giuliani, L., Ranee, A., Pacificr, G.M., 2000. Uridine 5'-
850 Diphosphoglucuronic acid (UDPGLcUA) in the human fetal liver , kidney and
851 placenta. *Eur. J. Drug Metab. Pharmacokinet.* 25, 161–163.

852 Clewell, H.J., Gearhart, J.M., Gentry, P.R., Covington, T.R., VanLandingham, C.B.,
853 Crump, K.S., Shipp, A.M., 1999. Evaluation of the uncertainty in an oral reference
854 dose for methylmercury due to interindividual variability in pharmacokinetics. *Risk*
855 *Anal.* 19, 547–558. doi:10.1023/A:1007017116171

856 Clewell, R.A., Clewell, H.J., 2008. Development and specification of physiologically
857 based pharmacokinetic models for use in risk assessment. *Regul. Toxicol.*
858 *Pharmacol.* 50, 129–43. doi:10.1016/j.yrtph.2007.10.012

859 Corbel, T., Perdu, E., Gayrard, V., Puel, S., Lacroix, M.Z., Viguié, C., Toutain, P.L.,
860 Zalko, D., Picard-Hagen, N., 2015. Conjugation and deconjugation reactions
861 within the fetoplacental compartment in a sheep model: A key factor determining
862 bisphenol a fetal exposure. *Drug Metab. Dispos.* 43, 467–476.
863 doi:10.1124/dmd.114.061291

864 Corley, R. a, Mast, T.J., Carney, E.W., Rogers, J.M., Daston, G.P., 2003. Evaluation of
865 physiologically based models of pregnancy and lactation for their application in
866 children's health risk assessments. *Crit. Rev. Toxicol.* 33, 137–211.
867 doi:10.1080/713611035

868 Coughlin, J.L., Thomas, P.E., Buckley, B., 2012. Inhibition of genistein glucuronidation
869 by bisphenol A in human and rat liver microsomes. *Drug Metab. Dispos.* 40, 481–
870 485. doi:10.1124/dmd.111.042366

871 Coughtrie, M.W., Burchell, B., Leakey, J.E., Hume, R., 1988. The inadequacy of
872 perinatal glucuronidation: immunoblot analysis of the developmental expression of
873 individual UDP-glucuronosyltransferase isoenzymes in rat and human liver
874 microsomes. *Mol. Pharmacol.* 34, 729–735.

875 Csanády, G., Oberste-Frielinghaus, H., Semder, B., Baur, C., Schneider, K., Filser, J.,
876 2002. Distribution and unspecific protein binding of the xenoestrogens bisphenol A
877 and daidzein. *Arch. Toxicol.* 76, 299–305. doi:10.1007/s00204-002-0339-5

878 Cubitt, H.E., Houston, J.B., Galetin, A., 2009. Relative Importance of Intestinal and
879 Hepatic Glucuronidation-Impact on the Prediction of Drug Clearance. *Pharm. Res.*
880 26, 1073–1083. doi:10.1007/s11095-008-9823-9

881 Davies, B., Morris, T., 1993. Physiological parameters in laboratory animals and
882 humans. *Pharm. Res.* doi:10.1023/A:1018943613122

883 Divakaran, K., Hines, R.N., McCarver, D.G., 2014. Human hepatic UGT2B15
884 developmental expression. *Toxicol. Sci.* 141, 292–299. doi:10.1093/toxsci/kfu126

885 Doerge, D.R., Twaddle, N.C., Vanlandingham, M., Brown, R.P., Fisher, J.W., 2011.
886 Distribution of bisphenol A into tissues of adult, neonatal, and fetal Sprague–
887 Dawley rats. *Toxicol. Appl. Pharmacol.* 255, 261–270.
888 doi:10.1016/j.taap.2011.07.009

889 Domoradzki, J.Y., Pottenger, L.H., Thornton, C.M., Hansen, S.C., Card, T.L., Markham,
890 D.A., Dryzga, M.D., Shiotsuka, R.N., Waechter, J.M., 2003. Metabolism and
891 pharmacokinetics of bisphenol A (BPA) and the embryo-fetal distribution of BPA
892 and BPA-monoglucuronide in CD Sprague-Dawley rats at three gestational
893 stages. *Toxicol. Sci.* 76, 21–34. doi:10.1093/toxsci/kfg206

894 Edginton, A.N., Ritter, L., 2009. Predicting plasma concentrations of bisphenol A in
895 children younger than 2 years of age after typical feeding schedules, using a
896 physiologically based toxicokinetic model. *Environ. Health Perspect.* 117, 645–
897 652. doi:10.1289/ehp.0800073

898 Edlow, A.G., Chen, M., Smith, N.A., Lu, C., McElrath, T.F., 2012. Fetal bisphenol A
899 exposure: Concentration of conjugated and unconjugated bisphenol A in amniotic
900 fluid in the second and third trimesters. *Reprod. Toxicol.* 34, 1–7.
901 doi:10.1016/j.reprotox.2012.03.009

902 EFSA, 2015. Scientific Opinion on the risks to public health related to the presence of
903 bisphenol A (BPA) in foodstuffs: Executive summary. *EFSA J.* 13, 4002.
904 doi:10.2903/j.efsa.2015.4002

905 Elsby, R., Maggs, J.L., Ashby, J., Park, B.K., 2001. Comparison of the modulatory
906 effects of human and rat liver microsomal metabolism on the estrogenicity of
907 bisphenol A: implications for extrapolation to humans. *J. Pharmacol. Exp. Ther.*
908 297, 103–113.

909 EU, 2003. European Union, Risk Assessment Report on 4,4'-isopropylidenediphenol
910 (bisphenol- A). *Eur. Chem. Bur.* 302.

911 Fetus, A.N.A., Sampling, W.S., Villus, C., Fluid, A., 1993. β -glucuronidase deficiency :
912 identification of an affected fetus with simultaneous sampling of chorionic villus

913 and amniotic fluid. *Prenat. Diagn.* 13, 429–433.

914 Fisher, J.W., Twaddle, N.C., Vanlandingham, M., Doerge, D.R., 2011. Pharmacokinetic
915 modeling: Prediction and evaluation of route dependent dosimetry of bisphenol A
916 in monkeys with extrapolation to humans. *Toxicol. Appl. Pharmacol.* 257, 122–
917 136. doi:10.1016/j.taap.2011.08.026

918 Gentry, P.R., Covington, T.R., Andersen, M.E., Clewell, H.J., 2002. Application of a
919 physiologically based pharmacokinetic model for isopropanol in the derivation of a
920 reference dose and reference concentration. *Regul. Toxicol. Pharmacol.* 36, 51–
921 68. doi:S0273230002915400 [pii]

922 Gentry, P.R., Covington, T.R., Clewell, H.J., 2003. Evaluation of the potential impact of
923 pharmacokinetic differences on tissue dosimetry in offspring during pregnancy and
924 lactation. *Regul. Toxicol. Pharmacol.* 38, 1–16. doi:10.1016/S0273-
925 2300(03)00047-3

926 Gerona, R.R., Woodruff, T.J., Dickenson, C.A., Pan, J., Jackie, M., Sen, S., Friesen,
927 M.M., Fujimoto, V.Y., Hunt, P.A., 2014. California population 47.
928 doi:10.1021/es402764d.Bisphenol-A

929 Ginsberg, G., Rice, D.C., 2009. Does rapid metabolism ensure negligible risk from
930 bisphenol A? *Environ. Health Perspect.* 117, 1639–1643.
931 doi:10.1289/ehp.0901010

932 Gundert-Remy, U., Mielke, H., Bernauer, U., 2013. Commentary: Dermal penetration of
933 bisphenol A-Consequences for risk assessment. *Toxicol. Lett.* 217, 159–161.
934 doi:10.1016/j.toxlet.2012.12.009

935 Hanioka, N., Naito, T., Narimatsu, S., 2008. Human UDP-glucuronosyltransferase
936 isoforms involved in bisphenol A glucuronidation. *Chemosphere* 74, 33–36.
937 doi:10.1016/j.chemosphere.2008.09.053

938 Hanioka, N., Oka, H., Nagaoka, K., Ikushiro, S., Narimatsu, S., 2011. Effect of UDP-
939 glucuronosyltransferase 2B15 polymorphism on bisphenol A glucuronidation.
940 *Arch. Toxicol.* 85, 1373–1381. doi:10.1007/s00204-011-0690-5

941 ICRP, 2002. Basic anatomical and physiological data for use in radiological protection:
942 reference values. *Ann. ICRP* 32, 1–277. doi:10.1016/S0146-6453(03)00002-2

943 Ikezuki, Y., Tsutsumi, O., Takai, Y., Kamei, Y., Taketani, Y., 2002. Determination of

944 bisphenol A concentrations in human biological fluids reveals significant early
945 prenatal exposure. *Hum. Reprod.* 17, 2839–2841. doi:10.1093/humrep/17.11.2839

946 Kaddar, N., Harthé, C., Déchaud, H., Mappus, E., Pugeat, M., 2008. Cutaneous
947 penetration of bisphenol A in pig skin. *J. Toxicol. Environ. Health. A* 71, 471–3.
948 doi:10.1080/15287390801906824

949 Kawade, N., Onishi, S., 1981. The prenatal and postnatal development of UDP-
950 glucuronyltransferase activity towards bilirubin and the effect of premature birth on
951 this activity in the human liver. *Biochem. J.* 196, 257–60.

952 Kawamoto, Y., Matsuyama, W., Wada, M., Hishikawa, J., Chan, M.P.L., Nakayama, A.,
953 Morisawa, S., 2007. Development of a physiologically based pharmacokinetic
954 model for bisphenol A in pregnant mice. *Toxicol. Appl. Pharmacol.* 224, 182–191.
955 doi:10.1016/j.taap.2007.06.023

956 Kim, Y.H., Kim, C.S., Park, S., Han, S.Y., Pyo, M.Y., Yang, M., 2003. Gender
957 differences in the levels of bisphenol A metabolites in urine. *Biochem. Biophys.*
958 *Res. Commun.* 312, 441–448. doi:10.1016/j.bbrc.2003.10.135

959 Kortejärvi, H., Urtti, A., Yliperttula, M., 2007. Pharmacokinetic simulation of biowaiver
960 criteria: The effects of gastric emptying, dissolution, absorption and elimination
961 rates. *Eur. J. Pharm. Sci.* 30, 155–166. doi:10.1016/j.ejps.2006.10.011

962 Kuester, R.K., Sipes, I.G., 2007. Prediction of Metabolic Clearance of Bisphenol A (4
963 ,4' -Dihydroxy- 2,2-diphenylpropane) using Cryopreserved Human Hepatocytes.
964 *Drug Metab. Dispos.* 35, 1910–1915. doi:10.1124/dmd.107.014787.

965 Kurebayashi, H., Okudaira, K., Ohno, Y., 2010. Species difference of metabolic
966 clearance of bisphenol A using cryopreserved hepatocytes from rats, monkeys
967 and humans. *Toxicol. Lett.* 198, 210–215. doi:10.1016/j.toxlet.2010.06.017

968 Kuroda, N., Kinoshita, Y., Sun, Y., Wada, M., Kishikawa, N., Nakashima, K., Makino,
969 T., Nakazawa, H., 2003. Measurement of bisphenol A levels in human blood
970 serum and ascitic fluid by HPLC using a fluorescent labeling reagent. *J. Pharm.*
971 *Biomed. Anal.* 30, 1743–1749. doi:10.1016/S0731-7085(02)00516-2

972 Kuruto-Niwa, R., Tateoka, Y., Usuki, Y., Nozawa, R., 2007. Measurement of bisphenol
973 A concentrations in human colostrum. *Chemosphere* 66, 1160–1164.
974 doi:10.1016/j.chemosphere.2006.06.073

- 975 Lassen, C., Mikkelsen, S.H., Brandt, U.K., Cowi, A.S., 2011. Migration of bisphenol A
976 from cash register receipts and baby dummies. *Surv. Chem. Consum. Prod.*
977 *Danish Minist. Environ.*
- 978 Lee, Y.J., Ryu, H.Y., Kim, H.K., Min, C.S., Lee, J.H., Kim, E., Nam, B.H., Park, J.H.,
979 Jung, J.Y., Jang, D.D., Park, E.Y., Lee, K.H., Ma, J.Y., Won, H.S., Im, M.W.,
980 Leem, J.H., Hong, Y.C., Yoon, H.S., 2008. Maternal and fetal exposure to
981 bisphenol A in Korea. *Reprod. Toxicol.* 25, 413–419.
982 doi:10.1016/j.reprotox.2008.05.058
- 983 Loccisano, A.E., Longnecker, M.P., Campbell, J.L., Andersen, M.E., Clewell, H.J.,
984 2013. Development of Pbpk Models for PFOA and PFOS for Human Pregnancy
985 and Lactation Life Stages. *J. Toxicol. Environ. Heal. Part A* 76, 25–57.
986 doi:10.1080/15287394.2012.722523
- 987 Longnecker, M.P., Harbak, K., Kissling, G.E., Hoppin, J.A., Eggesbo, M., Jusko, T.A.,
988 Eide, J., Koch, H.M., 2013. The concentration of bisphenol A in urine is affected
989 by specimen collection, a preservative, and handling. *Environ. Res.* 126, 211–214.
990 doi:10.1016/j.envres.2013.07.002
- 991 Lorber, M., Angerer, J., Koch, H.M., 2010. A simple pharmacokinetic model to
992 characterize exposure of Americans to Di-2-ethylhexyl phthalate. *J. Expo. Sci.*
993 *Environ. Epidemiol.* 20, 38–53. doi:10.1038/jes.2008.74
- 994 Lucier, W., Sonawane, B.R., 1977. Glucuronidation and deglucuronidation reactions in
995 hepatic and extrahepatic tissues during perinatal development. *Drug Metab.*
996 *Dispos.* 5, 279–287.
- 997 Martínez, M.A., Rovira, J., Sharma, R.P., Nadal, M., Schuhmacher, M., Kumar, V.,
998 2017. Prenatal exposure estimation of BPA and DEHP using integrated external
999 and internal dosimetry: A case study. *Environ. Res.* 158, 566–575.
1000 doi:10.1016/j.envres.2017.07.016
- 1001 Matysek, P., 1980. β -Glucuronidase Activity in Amniotic Fluid. *J. Clin. Chem. Clin.*
1002 *Biochem.* 18, 611–614.
- 1003 Mazur, C.S., Kenneke, J.F., Hess-Wilson, J.K., Lipscomb, J.C., 2010. Differences
1004 between human and rat intestinal and hepatic bisphenol a glucuronidation and the
1005 influence of alamethicin on in vitro kinetic measurements. *Drug Metab. Dispos.* 38,
1006 2232–2238. doi:10.1124/dmd.110.034819

- 1007 Mccance, R.A., Dean, R.F.A., Jones, P.E.H., 1949. The Glucuronide-synthesizing
1008 System in the Mouse and its Relationship to β -Glucuronidase. *Biochem. J.* 45,
1009 496–499.
- 1010 McLaughlin, B.E., Hutchinson, J.M., Graham, C.H., Smith, G.N., Marks, G.S., Nakatsu,
1011 K., Brien, J.F., 2000. Heme oxygenase activity in term human placenta. *Placenta*
1012 21, 870–873. doi:10.1053/plac.2000.0574
- 1013 Mendum, T., Stoler, E., VanBenschoten, H., Warner, J.C., 2011. Concentration of
1014 bisphenol A in thermal paper. *Green Chem. Lett. Rev.* 4, 81–86.
1015 doi:10.1080/17518253.2010.502908
- 1016 Mielke, H., Gundert-Remy, U., 2012. Physiologically based toxicokinetic modelling as a
1017 tool to support risk assessment: Three case studies. *J. Toxicol.* 2012.
1018 doi:10.1155/2012/359471
- 1019 Mielke, H., Gundert-Remy, U., 2009. Bisphenol A levels in blood depend on age and
1020 exposure. *Toxicol. Lett.* 190, 32–40. doi:10.1016/j.toxlet.2009.06.861
- 1021 Mielke, H., Partosch, F., Gundert-Remy, U., 2011. The contribution of dermal exposure
1022 to the internal exposure of bisphenol A in man. *Toxicol. Lett.* 204, 190–198.
1023 doi:10.1016/j.toxlet.2011.04.032
- 1024 Morck, T.J., Sorda, G., Bechi, N., Rasmussen, B.S., Nielsen, J.B., Ietta, F., Rytting, E.,
1025 Mathiesen, L., Paulesu, L., Knudsen, L.E., 2010. Placental transport and in vitro
1026 effects of Bisphenol A. *Reprod. Toxicol.* 30, 131–137.
1027 doi:10.1016/j.reprotox.2010.02.007
- 1028 Moriyama, K., Tagami, T., Akamizu, T., Usui, T., Saijo, M., Kanamoto, N., Hataya, Y.,
1029 Shimatsu, A., Kuzuya, H., Nakao, K., 2002. Thyroid hormone action is disrupted
1030 by bisphenol A as an antagonist. *J. Clin. Endocrinol. Metab.* 87, 5185–5190.
1031 doi:10.1210/jc.2002-020209
- 1032 Muna S. Nahar, Chunyang Liao, Kurunthachalam Kannan, and D.C.D., 2013. Fetal
1033 Liver Bisphenol A Concentrations and Biotransformation Gene Expression Reveal
1034 Variable Exposure and Altered Capacity for Metabolism in Humans. *J. Biochem.*
1035 *Mol. Toxicol.* 27, 116–123. doi:10.1002/jbt
- 1036 Nachman, R.M., Hartle, J.C., Lees, P.S.J., Groopman, J.D., 2014. Early Life
1037 Metabolism of Bisphenol A: A Systematic Review of the Literature. *Curr. Environ.*
1038 *Heal. reports* 1, 90–100. doi:10.1007/s40572-013-0003-7

- 1039 Nishikawa, M., Iwano, H., Yanagisawa, R., Koike, N., Inoue, H., Yokota, H., 2010.
1040 Placental transfer of conjugated bisphenol A and subsequent reactivation in the
1041 rat fetus. *Environ. Health Perspect.* 118, 1196–1203. doi:10.1289/ehp.0901575
- 1042 O’Flaherty, E.J., Scott, W., Schreiner, C., Beliles, R.P., 1992. A physiologically based
1043 kinetic model of rat and mouse gestation: disposition of a weak acid. *Toxicol. Appl.*
1044 *Pharmacol.* 112, 245–56.
- 1045 Palanza, P., Howdeshell, K.L., Parmigiani, S., vom Saal, F.S., 2002. Exposure to a low
1046 dose of bisphenol A during fetal life or in adulthood alters maternal behavior in
1047 mice. *Environ. Health Perspect.* 110, 415–422. doi:10.1289/ehp.02110s3415
- 1048 Partosch, F., Mielke, H., Gundert-Remy, U., 2013. Functional UDP-
1049 glucuronyltransferase 2B15 polymorphism and bisphenol A concentrations in
1050 blood: Results from physiologically based kinetic modelling. *Arch. Toxicol.* 87,
1051 1257–1264. doi:10.1007/s00204-013-1022-8
- 1052 Patisaul, H.B., Todd, K.L., Mickens, J.A., Adewale, H.B., 2009. Impact of neonatal
1053 exposure to the ER α agonist PPT, bisphenol-A or phytoestrogens on
1054 hypothalamic kisspeptin fiber density in male and female rats. *Neurotoxicology* 30,
1055 350–357. doi:10.1016/j.neuro.2009.02.010
- 1056 Pelkonen, O., 1973. Drug metabolism in the human fetal liver. Relationship to fetal age.
1057 *Arch. Int. Pharmacodyn. Ther.* 202, 281–287.
- 1058 Pelkonen, O., Kaltiala, E.H., Larmi, T.K.I., Karki, N.T., 1973. Comparison of activities of
1059 drug-metabolizing enzymes in human fetal and adult livers. *Clin. Pharmacol. Ther.*
1060 14, 840–846.
- 1061 Rey, R., Lukas-Croisier, C., Lasala, C., Bedecarrás, P., 2003. AMH/MIS: What we
1062 know already about the gene, the protein and its regulation. *Mol. Cell. Endocrinol.*
1063 211, 21–31. doi:10.1016/j.mce.2003.09.007
- 1064 Rubin, B.S., Soto, A.M., 2009. Bisphenol A: Perinatal exposure and body weight. *Mol.*
1065 *Cell. Endocrinol.* 304, 55–62. doi:10.1016/j.mce.2009.02.023
- 1066 Schönfelder, G., Wittfoht, W., Hopp, H., Talsness, C.E., Paul, M., Chahoud, I., 2002.
1067 Parent bisphenol a accumulation in the human maternal-fetal-placental unit.
1068 *Environ. Health Perspect.* 110, 703–707. doi:10.1289/ehp.021100703
- 1069 Sharma, R.P., Schuhmacher, M., Kumar, V., 2017. Review on crosstalk and common

- 1070 mechanisms of endocrine disruptors: Scaffolding to improve PBPK/PD model of
1071 EDC mixture. *Environ. Int.* 99, 1–14. doi:10.1016/j.envint.2016.09.016
- 1072 Shin, B.S., Kim, C.H., Jun, Y.S., Kim, D.H., Lee, B.M., Yoon, C.H., Park, E.H., Lee,
1073 K.C., Han, S.-Y., Park, K.L., Kim, H.S., Yoo, S.D., 2004. Physiologically Based
1074 Pharmacokinetics of Bisphenol a. *J. Toxicol. Environ. Heal. Part A* 67, 1971–1985.
1075 doi:10.1080/15287390490514615
- 1076 Sisson, T.R., Lund, C.J., Whalen, L.E., Telek, A., 1959. The blood volume of infants. I.
1077 The full-term infant in the first year of life. *J. Pediatr.* 55, 163–79.
1078 doi:10.1016/S0022-3476(59)80084-6
- 1079 Snijder, C.A., Heederik, D., Pierik, F.H., Hofman, A., Jaddoe, V.W., Koch, H.M.,
1080 Longnecker, M.P., Burdorf, A., 2013. Fetal growth and prenatal exposure to
1081 bisphenol A: The generation R study. *Environ. Health Perspect.* 121, 393–396.
1082 doi:10.1289/ehp.1205296
- 1083 Sperker, B., Backman, J.T., Kroemer, H.K., 1997a. The role of beta-glucuronidase in
1084 drug disposition and drug targeting in humans. *Clin.Pharmacokinet.* 33, 18–31.
- 1085 Sperker, B., Mürdter, T.E., Schick, M., Eckhardt, K., Bosslet, K., Kroemer, H.K., 1997b.
1086 Interindividual variability in expression and activity of human beta-glucuronidase in
1087 liver and kidney: consequences for drug metabolism. *J. Pharmacol. Exp. Ther.*
1088 281, 914–20.
- 1089 Strassburg, C.P., Strassburg, a, Kneip, S., Barut, a, Tukey, R.H., Rodeck, B., Manns,
1090 M.P., 2002. Developmental aspects of human hepatic drug glucuronidation in
1091 young children and adults. *Gut* 50, 259–65. doi:10.1136/gut.50.2.259
- 1092 Teeguarden, J.G., Twaddle, N.C., Churchwell, M.I., Doerge, D.R., 2016. Urine and
1093 serum biomonitoring of exposure to environmental estrogens I: Bisphenol A in
1094 pregnant women. *Food Chem. Toxicol.* 92, 129–142.
1095 doi:10.1016/j.fct.2016.03.023
- 1096 Teeguarden, J.G., Twaddle, N.C., Churchwell, M.I., Yang, X., Fisher, J.W., Seryak,
1097 L.M., Doerge, D.R., 2015. 24-hour human urine and serum profiles of bisphenol A:
1098 Evidence against sublingual absorption following ingestion in soup. *Toxicol. Appl.*
1099 *Pharmacol.* 288, 131–142. doi:10.1016/j.taap.2015.01.009
- 1100 Thayer, K.A., Doerge, D.R., Hunt, D., Schurman, S.H., Twaddle, N.C., Churchwell,
1101 M.I., Garantziotis, S., Kissling, G.E., Easterling, M.R., Bucher, J.R., Birnbaum,

- 1102 L.S., 2015. Pharmacokinetics of bisphenol A in humans following a single oral
1103 administration. *Environ. Int.* 83, 107–115. doi:10.1016/j.envint.2015.06.008
- 1104 Trdan Lusin, T., Roskar, R., Mrhar, A., 2012. Evaluation of bisphenol A glucuronidation
1105 according to UGT1A1*28 polymorphism by a new LC-MS/MS assay. *Toxicology*
1106 292, 33–41. doi:10.1016/j.tox.2011.11.015
- 1107 Vafeiadi, M., Roumeliotaki, T., Myridakis, A., Chalkiadaki, G., Fthenou, E., Dermitzaki,
1108 E., Karachaliou, M., Sarri, K., Vassilaki, M., Stephanou, E.G., Kogevinas, M.,
1109 Chatzi, L., 2016. Association of early life exposure to bisphenol A with obesity and
1110 cardiometabolic traits in childhood. *Environ. Res.* 146, 379–387.
1111 doi:10.1016/j.envres.2016.01.017
- 1112 Vandenberg, L.N., Chahoud, I., Heindel, J.J., Padmanabhan, V., Paumgarten, F.J.R.,
1113 Schoenfelder, G., 2010. Urinary, circulating, and tissue biomonitoring studies
1114 indicate widespread exposure to bisphenol A. *Environ. Health Perspect.* 118,
1115 1055–1070. doi:10.1289/ehp.0901716
- 1116 VandeVoort, C.A., Gerona, R.R., vom Saal, F.S., Tarantal, A.F., Hunt, P.A.,
1117 Hillenweck, A., Zalko, D., 2016. Maternal and Fetal Pharmacokinetics of Oral
1118 Radiolabeled and Authentic Bisphenol A in the Rhesus Monkey. *PLoS One* 11,
1119 e0165410. doi:10.1371/journal.pone.0165410
- 1120 Völkel, W., Bittner, N., Dekant, W., 2005. Quantitation of Bisphenol a and Bisphenol a
1121 Glucuronide in Biological Samples By High Performance Liquid Chromatography-
1122 Tandem Mass Abstract : *Drug Metab Dispos* 33, 1748–1757.
1123 doi:10.1124/dmd.105.005454.unintentionally
- 1124 Völkel, W., Colnot, T., Csanády, G.A., Filser, J.G., Dekant, W., 2002. Metabolism and
1125 kinetics of bisphenol a in humans at low doses following oral administration.
1126 *Chem. Res. Toxicol.* 15, 1281–1287. doi:10.1021/tx025548t
- 1127 Wang, J., Sun, B., Hou, M., Pan, X., Li, X., 2012. The environmental obesogen
1128 bisphenol A promotes adipogenesis by increasing the amount of 11 β -
1129 hydroxysteroid dehydrogenase type 1 in the adipose tissue of children. *Int. J.*
1130 *Obes.* 999–1005. doi:10.1038/ijo.2012.173
- 1131 WHO, F. and A.O. of the U.N., 2010. Toxicological and Health Aspects of Bisphenol A.
1132 *World Heal. Organ.* 60.
- 1133 Xi, W., Lee, C.K.F., Yeung, W.S.B., Giesy, J.P., Wong, M.H., Zhang, X., Hecker, M.,

- 1134 Wong, C.K.C., 2011. Effect of perinatal and postnatal bisphenol A exposure to the
1135 regulatory circuits at the hypothalamus-pituitary-gonadal axis of CD-1 mice.
1136 *Reprod. Toxicol.* 31, 409–417. doi:10.1016/j.reprotox.2010.12.002
- 1137 Yang, X., Doerge, D.R., Fisher, J.W., 2013. Prediction and evaluation of route
1138 dependent dosimetry of BPA in rats at different life stages using a physiologically
1139 based pharmacokinetic model. *Toxicol. Appl. Pharmacol.* 270, 45–59.
1140 doi:10.1016/j.taap.2013.03.022
- 1141 Yang, X., Doerge, D.R., Teeguarden, J.G., Fisher, J.W., 2015. Development of a
1142 physiologically based pharmacokinetic model for assessment of human exposure
1143 to bisphenol A. *Toxicol. Appl. Pharmacol.* 289, 442–456.
1144 doi:10.1016/j.taap.2015.10.016
- 1145 Yang, X., Fisher, J.W., 2015. Unraveling bisphenol A pharmacokinetics using
1146 physiologically based pharmacokinetic modeling. *Front. Pharmacol.* 6, 1–7.
1147 doi:10.3389/fphar.2015.00292
- 1148 Ye, X., Zhou, X., Hennings, R., Kramer, J., Calafat, A.M., 2013. Potential External
1149 Contamination with Bisphenol A and Other Ubiquitous Organic Environmental
1150 Chemicals during Biomonitoring Analysis: An Elusive Laboratory Challenge.
1151 *Environ. Health Perspect.* 121, 283–286. doi:10.1289/ehp.1206093
- 1152 Yoon, M., Efremenko, A., Blaauboer, B.J., Clewell, H.J., 2014. Evaluation of simple in
1153 vitro to in vivo extrapolation approaches for environmental compounds. *Toxicol.*
1154 *Vitr.* 28, 164–170. doi:10.1016/j.tiv.2013.10.023
- 1155 Zalko, D., Jacques, C., Duplan, H., Bruel, S., Perdu, E., 2011a. Viable skin efficiently
1156 absorbs and metabolizes bisphenol A. *Chemosphere* 82, 424–430.
1157 doi:10.1016/j.chemosphere.2010.09.058
- 1158 Zalko, D., Jacques, C., Duplan, H., Bruel, S., Perdu, E., 2011b. Viable skin efficiently
1159 absorbs and metabolizes bisphenol A. *Chemosphere* 82, 424–430.
1160 doi:10.1016/j.chemosphere.2010.09.058
- 1161 Zhang, J., Cooke, G.M., Curran, I.H.A., Goodyer, C.G., Cao, X.L., 2011. GC-MS
1162 analysis of bisphenol A in human placental and fetal liver samples. *J. Chromatogr.*
1163 *B Anal. Technol. Biomed. Life Sci.* 879, 209–214.
1164 doi:10.1016/j.jchromb.2010.11.031
- 1165 Zhang, T., Sun, H., Kannan, K., 2013. Blood and urinary bisphenol a concentrations in

1166 children, adults, and pregnant women from China: Partitioning between blood and
1167 urine and maternal and fetal cord blood. *Environ. Sci. Technol.* 47, 4686–4694.
1168 doi:10.1021/es303808b

1169

1170

1171

1172

1173

1174

1175

1176

1177

1178

Figure Labels

Figure 1 Conceptual model for the development of P-PBPK model. It involves the development of adult PBPK model and extension of this model to P-PBPK model with the addition of placenta and fetus sub-compartment. **K = partition coefficient and subscripts L = Liver, B= blood, K= kidney, T= testis, S= skin, R= rest organ, G= gut.**

Figure 2. The pharmacokinetic of BPA and its conjugate in both mother and fetus. The placental-fetal unit assumes a bidirectional transfer process of BPA and BPA-C describing distribution of BPA and its metabolites in mother and fetus body.

Figure 3. Concentration–time profiles after oral dosing of adult females (n = 7) with 100 µg/kg of deuterated BPA (d6-BPA) (Thayer et al., 2015). A) Simulated individual (solid colour lines) and observed individual plasma (dot points) d6-BPA concentrations; B) Simulated individual (solid colour lines) and observed individual plasma (dot points) d6-BPAG concentrations; C) Simulated individual (solid colour lines) and observed individual plasma (dot points) d6-BPAS concentrations. Simulations of individual patients were performed using individual body weights and their fat content while keeping other model parameters constant.

Figure 4. Observed vs predicted mother plasma and fetus plasma of volunteer participated in Schönfelder et al. (2002) study for 32 to 41th week of GA; box plot containing mean (red diamond), median (horizontal line of boxplot), highest (upper bar of boxplot), lowest (lower bar of boxplot) value and observed value marked as black star.

Figure 5. Predicted mother plasma and fetus plasma for low dose scenario, estimated from the Ikezuki et al. (2002) mother plasma concentration, for 32 to 41th week of GA; box plot containing mean (red diamond), median (horizontal line of boxplot), highest (upper bar of boxplot), and lowest (lower bar of boxplot) value.

Figure 6. Observed vs predicted placenta and fetal liver for higher exposure scenario for 11 to 22nd week of GA; box plot containing mean (red diamond), median (horizontal line of boxplot), highest (upper bar of boxplot), lowest (lower bar of boxplot) and observed value (Zhang et al., 2011) marked as green star.

Figure 7. Simulated low dose exposure scenario for amniotic BPA concentration starting from early mid-gestational to late gestational period (blue line curve) vs. observed (mean \pm SD) concentration in Ikezuki et al. (2002) studied during 15-18 and 32-40 weeks of pregnancy (red error bar).

Figure 8. Simulated mean \pm SD of BPA for two exposure scenario (high and low dose) for the period of 32-40 GA and the observed mean \pm SD of BPA in different studies for both mother and fetus BPA plasma concentration.